ENCLOSURE 2

MFN 05-115

Revised DCD Sections:

4.2, "Fuel System Design"

4.3, "Nuclear Design"

4.4, "Thermal and Hydraulic Design"

(Conditional Release – pending closure of design verifications)

4.2 FUEL SYSTEM DESIGN

The fuel system is defined as consisting of the fuel assembly and the reactivity control assembly. The fuel assembly is comprised of the fuel bundle, channel and channel fastener. The fuel bundle is comprised of fuel rods, water rods, and fuel rods containing burnable neutron absorber, spacers, springs and assembly fittings. Appendix 4B contains a set of design criteria to be satisfied by new fuel designs to loaded in the ESBWR.

To demonstrate the ESBWR system response in this DCD Tier 2, a reference core, based upon a current NRC-approved GE14 fuel design, is modified to account for the shorter active fuel length. The latest GE14 information is provided in the most recent revision of the GE Fuel Bundle Designs Report and its supplements (Reference 4.2-1).

This section addresses the reactivity control elements that extend from the coupling interface of the control rod drive mechanism (per Regulatory Guide 1.70). The functional design of the reactivity control system is detailed in Section 4.6. The control rod design to be used in an ESBWR is any design that meets the criteria documented in Appendix 4C.

The following subsection provides the fuel system design bases and design limits. It is consistent with the criteria of the Standard Review Plan, Section 4.2.

4.2.1 Design Bases

4.2.1.1 Fuel Assembly

The fuel assembly (comprised of the fuel bundle, channel and channel fastener) is designed in compliance with requirements of 10 CFR 20, 10 CFR 50 and 10 CFR 100 to ensure that possible fuel damage would not result in the release of radioactive materials in excess of prescribed limits, and that fuel assembly coolability is maintained during postulated accidents. The core nuclear and hydraulic characteristics, plant equipment characteristics, and instrumentation and protection systems are evaluated to assure that this requirement is met.

The thermal-mechanical design process emphasizes that:

- The fuel assembly provides substantial fission products retention capability during all potential operational modes
- The fuel assembly provides sufficient structural integrity to prevent operational impairment of any reactor safety equipment

The fuel assembly and its components are designed to withstand:

- The predicted thermal, pressure and mechanical interaction loadings occurring during startup testing, normal operation, and anticipated operational occurrences, infrequent incidents and accidents
- Loading predicted to occur during handling

Steady-state operating limits are established to ensure that actual fuel operation, including anticipated operational occurrences (AOOs), is maintained within the fuel rod thermal-mechanical design bases. These operating limits define the maximum allowable fuel pellet operating power level as a function of fuel pellet exposure in terms of Maximum Linear Heat

Generation Rate (MLHGR). Lattice local power and exposure distributions are applied in the determination of the MLHGR limits.

The detailed design bases for each of the fuel assembly damage, fuel rod failure and fuel assembly cooling criteria are defined in Section II.A of Standard Review Plan 4.2 (except control rod reactivity; see Subsection 4.2.1.2) and are provided in Section 4B.2 of Appendix 4B.

4.2.1.1.1 Fuel Temperature

The fuel rod centerline temperature is limited to ensure with high probability that fuel rod failure due to fuel melting will not occur during normal operation, including AOOs.

4.2.1.1.2 Fuel Rod Internal Pressure

During fabrication, the fuel rod is filled with helium to a specified pressure. With the initial rise to power, this fuel rod internal pressure increases due to the corresponding increase in the gas average temperature and the reduction in the fuel rod void volume due to fuel pellet expansion and inward cladding elastic deflection due to the higher reactor coolant pressure. With continued irradiation, the fuel rod internal pressure will progressively increase further due to the release of gaseous fission products from the fuel pellets to the fuel rod void volume. With sufficient irradiation, a potential adverse thermal feedback condition may arise due to excessive fuel rod internal pressure.

When the internal pressure exceeds the reactor coolant pressure, the cladding will deform outward (cladding creepout). If the rate of this cladding outward deformation exceeds the rate at which the fuel pellet expands due to irradiation (fission product) swelling (fuel swelling rate), the pellet-cladding gap will begin to open (or increase if the gap is already open). An increase in the pellet-cladding gap will reduce the pellet-cladding thermal conductance thereby increasing fuel temperatures. The increased fuel temperatures will result in further fuel pellet fission gas release, greater fuel rod internal pressure, and correspondingly a faster rate of cladding outward deformation and gap opening.

This potential thermal feedback condition is avoided by limiting the cladding creepout rate, due to fuel rod internal pressure, to less than or equal to the fuel pellet irradiation swelling rate.

4.2.1.1.3 Cladding Strain

The fuel rod cladding strain is limited to ensure that fuel rod failure due to pellet-clad mechanical interaction will not occur. To achieve this objective the calculated cladding circumferential plastic strain is limited to less than 1% during anticipated operational occurrences.

4.2.1.1.4 Cladding Corrosion and Corrosion Product Buildup

Zircaloy cladding tubes undergo oxidation at slow rates during normal reactor operation and reactor water corrosion products (crud) are deposited on the cladding outside surface (see Reference 4.2-2). The cladding oxidation causes thinning of the cladding tube wall and introduces a resistance to the fuel rod-to-coolant heat transfer. Crud buildup can also introduce a resistance to heat transfer. The expected extent of the oxidation and the buildup of the corrosion products is specifically considered in the fuel rod design analyses. Thus the impacts of the temperature increase correspondingly altered material properties and the cladding wall thickness thinning resulting from cladding corrosion on fuel rod behavior relative to impacted design

criteria (such as fuel temperature and cladding strain) are explicitly addressed. The oxide thickness itself is not separately limiting and no direct design limit on cladding oxide thickness is therefore specified.

4.2.1.1.5 Fuel Rod Hydrogen Absorption

There are two considerations relative to fuel rod hydrogen absorption. The first consideration involves the potential for hydrogenous impurity evolution, historically from the fuel pellets, resulting in primary hydriding and fuel rod failure. This consideration is addressed by the application of a fabrication specification limit of 1 ppm hydrogen on the as-fabricated fuel pellets. The absence of primary-hydriding induced fuel rod failures demonstrates the effectiveness of this limit since its first application in 1972. The second consideration is the partial absorption by the fuel rod cladding of hydrogen liberated by the cladding waterside corrosion reaction. Mechanical properties testing demonstrates that the cladding mechanical properties are unaffected for hydrogen contents far in excess of that experienced during normal operation. On this basis, there is no specific design criterion applied to the cladding hydrogen content.

4.2.1.1.6 Cladding Creep Collapse

The fuel rod is evaluated to ensure that fuel rod failure due to cladding collapse into a fuel column axial gap will not occur. This criterion is discussed in detail in Reference 4.2-3.

4.2.1.1.7 Fuel Rod Stresses

Based upon the limits specified in ANSI/ANS 57.5-1981, the fuel rod is evaluated to ensure that the fuel will not fail due to cladding stresses or strains exceeding the cladding ultimate stress or strain capability. The figure of merit employed is termed the Design Ratio, where:

$$\text{Design Ratio} = \frac{\text{Effective Stress}}{\text{Stress Limit}} \text{ or } \frac{\text{Effective Strain}}{\text{Strain Limit}}$$

The effective stress or strain is determined applying the distortion energy theory. The limit is the material ultimate stress or strain. The limit used is that the Design Ratio must be less than or equal to 1.0.

4.2.1.1.8 Dynamic Loads / Cladding Fatigue

The fuel rod is evaluated to ensure that cladding strains due to cyclic loadings will not exceed the cladding material fatigue capability. The design limit for fatigue cycling is determined from Zircaloy fatigue experiments and is conservatively specified to ensure with high confidence that failure by cladding fatigue will not occur. Based on the LWR cyclic design basis presented in Reference 4.2-4, the cladding fatigue life usage is calculated and maintained below the cladding material fatigue limit.

As noted in Section 4.2.1.1, for each fuel design, steady-state operating limits are established to ensure that actual fuel operation, including AOOs, complies with the fuel rod thermal–mechanical design and safety analysis bases above. These operating limits define the maximum allowable fuel pellet operating power level as a function of fuel pellet exposure. Lattice local power and exposure peaking factors may be applied to transform the maximum allowable fuel

pellet power level into Maximum Linear Heat Generation Rate (MLHGR) limits for individual fuel bundle designs.

4.2.1.2 Control Rods

The control rod is designed to have:

- Sufficient mechanical strength to prevent displacement of its reactivity control material
- Sufficient mechanical strength to prevent deformation that could inhibit its motion
- Sufficient mechanical strength to prevent damage during potential interference with fuel channel(s)

The detailed design bases for the control rod are provided in Appendix 4C.

Typical control rod patterns and associated power distribution for an ESBWR are provided in Appendix 4A.

4.2.2 Description and Design Drawings

4.2.2.1 Fuel Assembly

The components of the reference fuel assembly (GE14E) are shown in Figure 4.2-2, and consist of a fuel bundle, a channel that surrounds the fuel bundle, and a channel fastener that attaches the bundle to the channel. The fuel and water rods are spaced and supported by upper and lower tieplates and intermediate spacers. The lower tieplate has a nosepiece that has the function of supporting the fuel assembly in the reactor. The upper tieplate has a handle for transferring the fuel bundle from one location to another. The identifying fuel assembly serial number is engraved on the top of the handle; no two assemblies bear the same serial number. A boss projects from one side of the handle to ensure proper orientation of the assembly in the core. Finger springs are located between the lower tieplate and channel and are utilized to control the bypass flow through that flow path. The difference between GE14E and GE14C is shown in Reference 4.2-4.

4.2.2.1.1 Fuel Rods

Each fuel rod consists of high–density ceramic uranium dioxide fuel pellets stacked within Zircaloy cladding that is evacuated, backfilled with helium and sealed with Zircaloy end plugs welded on each end. A thin zirconium barrier liner is metallurgically bonded to the innermost part of the Zircaloy cladding during cladding fabrication. Three types of fuel rods are used in a fuel bundle; tie rods, standard rods, and partial length rods. The tie rods in each fuel bundle have lower end plugs that thread into the lower tieplate and threaded upper end plugs that extend through the upper tieplate. A nut and locking tab are installed on the upper end plug to hold the fuel bundle together. The tie rods support the weight of the assembly during fuel lifting operations. During normal reactor operation, the assembly is supported by the lower tieplate.

The end plugs of the standard rods have shanks that fit into bosses in the tieplates. An expansion spring is located over the upper end plug shank of each rod in the bundle to keep the rods seated in the lower tieplate.

The partial length rods are installed to reduce the bundle pressure drop and have lower end plugs that thread into the lower tieplate, similar to the tie rods. The upper endplugs do not extend to the upper tieplate and are only used to seal the top end of the partial length rods.

Each fuel rod contains high-density ceramic uranium dioxide fuel pellets stacked within Zircaloy cladding. The fuel rod is evacuated, backfilled with helium, and sealed with end plugs welded into each end. U-235 enrichments may vary axial within a fuel rod and from fuel rod to fuel rod within a bundle to reduce local peak-to-average fuel rod power ratios. Selected fuel rods within each bundle may include small amounts of gadolinium as a burnable poison.

Adequate free volume to accommodate gaseous fission products released from the fuel pellets during normal operation is provided within each fuel rod in the form of a pellet-to-cladding gap and a plenum region at the top of each fuel rod. A plenum spring, or retainer, is provided in the plenum space to minimize the movement of the column of fuel pellets inside the fuel rod during shipping and handling.

4.2.2.1.2 Water Rods

Water rods are hollow Zircaloy tubes with several holes around the circumference near each end to allow coolant to flow through the rod. One water rod in each bundle axially positions the spacers. This spacer–positioning water rod is designed with spacer positioning tabs that are welded to the tube exterior above and below each spacer location. An expansion spring is located between the water rod shoulder and upper tieplate to allow for differential axial expansion similar to the full–length fuel rods.

4.2.2.1.3 Fuel Spacer

The primary function of the spacer is to provide lateral support and maintain lateral spacing of the fuel rods, with consideration of thermal-hydraulic performance, fretting wear, strength, neutron economy, and manufacturability.

4.2.2.1.4 Upper and Lower Tieplates

Stainless steel upper and lower tieplates carry the weight of the fuel and position the rod ends laterally during operation and handling.

4.2.2.1.5 Finger Springs

Finger springs may be employed to control the bypass flow through the channel-to-lower tieplate flow path for some fuel assemblies.

4.2.2.1.6 Channels

The fuel channel is composed of a Zirconium based material or equivalent, and performs the following functions:

- Forms the fuel bundle flow path outer periphery for bundle coolant flow
- Provides surfaces for control rod guidance in the reactor core
- Provides structural stiffness to the fuel bundle sufficient to support lateral loadings applied from fuel rods through the fuel spacers

- Minimizes, in conjunction with finger springs (if present) and bundle lower tieplate, coolant bypass flow at the channel/lower tieplate interface
- Transmits fuel assembly seismic loadings to the core internal structure(fuel top guide and fuel support plate)
- Provides a heat sink during loss-of-coolant accident (LOCA)
- Provides a stagnation envelope for incore fuel sipping

The channel is open at the bottom and makes a sliding seal fit on the lower tieplate surface. The upper ends of the fuel assemblies in a four-bundle cell are positioned in the corners of the cell against the top guide beams by the channel fastener springs. At the top of the channel, two diagonally opposite corners have welded tabs which support the weight of the channel on the threaded raised posts of the upper tieplate. One of these raised posts has a threaded hole. The channel is attached to the fuel bundle using the threaded channel fastener assembly, which also includes the fuel assembly positioning spring. Channel-to-channel spacing is assured by the fuel bundle spacer buttons located on the upper portion of the channel adjacent to the control rod passage area.

4.2.2.2 Control Rods

The control rod assemblies (Figure 4.2-3) perform the functions of power shaping, reactivity control, and scram reactivity insertion for safety shutdown response. Power distribution in the core is controlled during operation of the reactor by manipulating selected patterns of control rods to counterbalance steam void effects at the top of the core.

The control rod main structure consists of a top handle, an absorber section, and a bottom connector assembled into a cruciform shape. The top handle contains a grapple opening for handling. The absorber section is an array of stainless steel tubes filled with boron carbide powder or a combination of boron carbide powder and hafnium rods. The connector is positioned on the bottom of the control rod for attachment to the control rod drive. While being inserted into the core, the control rod is restricted to the cruciform envelope created by the fuel bundles. The connector rollers guide the control rod within the guide tube as the control rod is inserted and withdrawn from the core. Detailed configuration of the control rod is shown in Figure 4.2-4.

4.2.3 Fuel Assembly Design Evaluations

4.2.3.1 Evaluation Methods

Most of the fuel rod thermal-mechanical design analyses are performed using the GSTRM (Reference 4.2-2). The GSTRM analyses are performed for the following conditions:

1. For each analysis, fuel rod input parameters are based on either the most unfavorable manufacturing tolerances (‘worst case’ analyses) or statistical distributions of the input values. Calculations are then performed to provide either a ‘worst case’ or statistically bounding tolerance limit for the resulting output parameter(s).

2. Operating conditions are postulated which cover the conditions anticipated during normal steady-state operation and anticipated operational occurrences.

The first step in the fuel rod design evaluations is to establish an upper bound power history envelope for the different fuel rod types, e.g. limiting power histories as a function of the peak exposure in the fuel rod. These power histories are then used for all fuel rod thermal-mechanical design analyses to evaluate the fuel rod design features and demonstrate conformance to the design criteria. These power histories are also applied as a design constraint to the reference core loading nuclear design analyses.

In the GSTRM analyses it is assumed that the fuel rod (axial) node with the highest power operates on the limiting power-exposure envelope during its entire operating lifetime. The axial power distribution is changed three times during each operating cycle (BOC, MOC and EOC), to assure conservative prediction of the release of gaseous fission products from the fuel pellets to the rod free volume. The relative axial power distributions used for a standard fuel rod are shown in Figure 4.2-1.

4.2.3.1.1 Worst Tolerance Analyses

The analyses performed to evaluate the cladding circumferential plastic strain during an anticipated operational occurrence applies worst tolerance assumptions. In this case, the GSTRM inputs important to this analysis are all biased to the fabrication tolerance extreme in the direction that produces the most severe result. The biases are discussed in detail in Reference 4.2-5.

4.2.3.1.2 Statistical Analyses

The remaining GSTRM analyses are performed using standard error propagation statistical methods. The statistical analysis procedure is presented in Reference 4.2-5.

4.2.3.2 Cladding Plastic Strain

This analysis is also performed using the GSTRM code and the worst-tolerance methodology noted above. For each fuel rod type the cladding plastic strain is calculated at different exposure points, whereby an overpower is assumed relative to the limiting power history. At the most limiting exposure point, the magnitude of the overpower event is further increased until the cladding plastic strain approaches 1%. The result from this analysis is used to establish the Mechanical Overpower (MOP) discussed below.

4.2.3.3 Fuel Rod Internal Pressure

This analysis is performed using the GSTRM code and the statistical methodology noted above. Values for the fuel rod internal pressure average value and standard deviation are determined at different fuel rod exposure points. At each of these exposure points, the fuel rod internal pressure required to cause the cladding to creep outward at a rate equal to the fuel pellet irradiation swelling rate is also determined using the same method. Based on the two calculated distributions a design ratio ‘cladding creepout rate – to – fuel swelling rate’ is determined such that, with at least 95% confidence, the fuel rod cladding will not creep out at a rate greater than the fuel pellet irradiation swelling rate.

4.2.3.4 Fuel Pellet Temperature

This analysis is performed statistically using the GSTRM code. For each fuel rod type the fuel pellet center temperature is statistically calculated at different exposure points, whereby an overpower is assumed relative to the limiting power history. At the most limiting exposure point, the magnitude of the overpower event is further increased until incipient fuel center-melting occurs. The result from this analysis establishes the Thermal Overpower (TOP) discussed below.

4.2.3.5 Cladding Fatigue Analysis

This analysis is performed statistically using the GSTRM code. For calculating the cladding fatigue, variations in power and coolant pressure, as well as coolant temperature, are superimposed on the limiting power history.

The fuel duty cycles shown in Reference 4.2-5 represent conservative assumptions regarding power changes anticipated during normal reactor operation including anticipated operational occurrences, planned surveillance testing, normal control blade maneuvers, shutdowns, and special operating modes such as daily load following. Based on these assumptions, the cladding strain cycles are analyzed as shown in Reference 4.2-5.

4.2.3.6 Cladding Creep Collapse

This analysis consists of a detailed finite element mechanics analysis of the cladding. This evaluation is described in detail in References 4.2-3 and 4.2-5.

4.2.3.7 Fuel Rod Stress Analysis

The fuel rod stress analysis is performed using the Monte Carlo statistical methodology and addresses local fuel rod stress concerns, such as the stresses at spacer contact points, that are not addressed by the GSTRM code. Results from GSTRM analyses are used to generate inputs for the stress analysis. The cladding stress analysis is described in detail in Reference 4.2-5.

4.2.3.8 Thermal and Mechanical Overpowers

As discussed above, analyses are performed to determine the values of the maximum overpower magnitudes that do not result in violation of the cladding circumferential plastic strain criterion (MOP-Mechanical Overpower) and the incipient fuel center-melting criterion (TOP-Thermal Overpower). Conformance to these criteria is demonstrated as a part of the normal core design and transient analysis process by comparison of the calculated core transient mechanical and thermal overpowers, as defined in Reference 4.2-5, to the mechanical and thermal overpower limits determined by the GSTRM analyses.

4.2.3.9 Fretting Wear

Testing is performed to assure that the mechanical features of the design, particularly those related to spacers and tie plates, do not result in significant vibration and consequent fretting wear, particularly at spacer –fuel rod contact points. The vibration response of the new design is compared to a design that has demonstrated satisfactory performance through discharge exposure.

4.2.3.10 Water Rods

Calculations are performed to determine component stresses at the bounding load conditions and compared to applicable criteria, such as yield and ultimate stresses. The load conditions take into account shipping and handling loads, seismic induced bending moment, and the pressure differential across the water rod. The design is also evaluated using finite element analysis to determine the critical buckling load and insure adequacy relative to axial loads resulting from differential growth of water rods and other fuel assembly components.

4.2.3.11 Tie Plates

Adequacy of tie plate designs is demonstrated by detailed finite element analysis and/or mechanical testing for bounding fuel handling and seismic load conditions.

4.2.3.12 Spacers

Fuel spacer acceptability is proved by testing in accordance with NRC approved methods. The bounding load condition is seismic loading. Tests are conducted to demonstrate spacer fatigue capability and compliance with load limits and to demonstrate that a coolable geometry is maintained by showing minimal deformation at the combined load condition. Fretting wear is addressed by performing FIV tests and evaluating the results relative to spacer designs that have demonstrated acceptable performance.

4.2.3.13 Channel

Channel adequacy relative to applicable design criteria is conformed by performing the following evaluations:

- Calculation of elastic stress and deflection due to channel wall ΔP
- Calculation of thermal stresses due to the various temperature gradients to which the channel is subjected during normal operation and handling
- Calculations of fatigue and stress rupture that consider the combined effect of pressure-temperature cycling and hold time
- Elastic-plastic and creep calculations of channel wall permanent deflection
- Calculation of channel stress due to control rod contact
- Channel/lower tie plate differential thermal expansion analysis

4.2.3.14 Conclusions

The results for the analyses described above are presented in detail in References 4.2-4 and 4.2-5. In summary, the GE14 design for ESBWR operation meets all the criteria noted above, plus those that address accidents discussed in References 4.2-4 and 4.2-5.

4.2.4 Control Rods Design Evaluations

The control rod evaluation methods described in Section 4C.2 is used established methodology for the control rod. The evaluation methodology history demonstrates that the criteria of

Appendix 4C are satisfactory for the Marathon control rod. The Marathon control rods for ESBWR is based on the Marathon control rod design for BWR/2 through BWR/6, which have been applied and licensed and applied to actual plants [Reference. 4.2-7]. Where the BWR/2 through BWR/6 was not adequate to apply to ESBWR, the ABWR evaluation is used.

4.2.4.1 SCRAM

The dynamic loads on the control rods are bounded by the fine motion control rod drive (FMCRD) imposed loads (scram loads) in the vertical direction. The ESBWR inoperative buffer loads are the highest vertical loads experienced by the control rod due to the high terminal velocity. The control rod is evaluated using a dynamic analysis in reference 4.2-8. A model of mass, springs and gap elements is used to simulate a detailed representation of all the load bearing components of the assembly during a scram event. The computer program runs the model at cold temperatures speeds and properties as well as elevated temperature speeds and properties. The resultant loads are evaluated using the material properties and geometry for the area subject to the load. The effective stress is determined using the distortion energy theory. The limit is the material ultimate stress or strain. Based on the reactor cycle the loads are then evaluated for fatigue in reference 4.2-8. The fatigue usage is evaluated against a limit of 1.0.

4.2.4.2 Seismic

Fuel channel deflections, which result from seismic and LOCA events impose lateral loads on the controls rods. The Marathon control rod is analyzed for Operating Basis Earthquake (OBE) events and Safe Shutdown Earthquake (SSE) events, reference 4.2-8. The BWR/2 through 6 and the ABWR have similar channel lengths and deflections. Due to the shorter length of the ESBWR channel with the same relative cross section, the expected deflection is less.

The OBE analysis is normally performed by evaluating the strain in the Marathon absorber section when deflected 20 to 24 mm. The absorber section strain has been analyzed for channel deflections exceeding 24 mm and found to be acceptable, reference 4.2-8.

The SSE analysis is performed through testing to show full insertion during fuel channel deflections. For example, testing was performed on the ABWR Marathon to confirm seismic scramability. The ABWR Marathon was tested at amplitudes of 10, 20, 30 and 40mm. The scram times were found to be acceptable and the control rod was not damaged. The ESBWR channels will be shorter making the fuel assembly stiffer and the fuel channel lateral deflections less. The increase in system stiffness offset by the decrease in lateral deflection make the ABWR Marathon seismic scramability test representative of the ESBWR conditions, reference 4.2-8.

4.2.4.3 Stuck Rod

Compression due to a stuck rod at the time of scram is controlled by the FMCRD. Assuming the FMCRD will exert the same compression loads, the shorter ESBWR control rod buckling is acceptable, even for one wing, reference 4.2-8.

4.2.4.4 Absorber Burn-Up Related Loads

The absorber containment licensed in reference 4.2-7 is applicable to the ESBWR Marathon. The same methodology is used for ESBWR Marathon in reference 4.2-8. The square tube

designed accommodates loads created by the neutron irradiation of the absorber material. In the case of B4C powder, tube wall stresses due to helium gas generation, B4C swelling, and moisture vapor heat-up are considered. The stress due to helium pressure and strain due to B4C swelling are adequate for the nuclear design life of the control rod.

4.2.4.5 Handling Loads

The ESBWR Marathon is designed to accommodate three times the weight of the control rod, reference 4.2-8.

4.2.4.6 Hydraulics

Inspection experience over 13 years has shown the Marathon control rod is not damaged by the vibrations or cavitations set up by coolant velocities and velocity distributions in the bypass region between fuel channels, reference 4.2-8.

4.2.4.7 Materials

Materials selected for use in the Marathon control rod components are chosen to minimize the component end-of-life radioactivity in order to reduce personnel exposure during handling on-site, and for final off-site shipping and burial, reference 4.2-8. All Marathon control rod materials are less than <.03 weight percent cobalt. The average niobium content for the handle and absorber section less boron carbide and hafnium is < 0.1 weight percent.

4.2.4.8 Nuclear Performance

The nuclear lifetime of the initial ESBWR Marathon control rod type will be established as 10 percent reduction in reactivity worth (Dk/k) in any quarter axial segment, reference 4.2-9. Subsequent Marathon designs or absorber section loadings will be within +/-5%Dk/k of the initial Marathon design.

Similar to what has been provided to US BWRs over the last 17 years, additional type Marathon control rods may be supplied with a different absorber configurations allowing higher reactivity worth and larger relative allowable decrease with respect to the initial Marathon control rod type's 10 percent reduction.

4.2.4.9 Mechanical Compatibility

Similar to the control rods supplied to ABWR and BWR/2 through BWR/6, the ESBWR Marathon control rod is designed to be compatible with interfaces.

The ESBWR Marathon is designed to be compatible with the guide tube cylindrical boundary, provides a seat with the guide tube base during Fine Motion Control Rod Drive (FMCRD) removal, provides lower guide rollers for smooth transitions, and clearance with the orificed fuel support for insertion and withdrawal from the core.

The control rod coupling socket provides a compatible interface with the FMCRD. The coupling engages the FMCRD by rotating one-eighth turn (45°). With the FMCRD, control rod drive housing, and CRGT positively assembled, any orientation of the cruciform control rod between the fuel assemblies shall be a coupled position, and rotation to an uncoupled position shall not be

possible during reactor operation. The four lobes of the FMCRD coupling spud are in line with the four wings of the control rod in the coupled position.

The control rod is designed to permit coupling and uncoupling of the control rod drive from below the vessel for FMCRD servicing without necessitating the removal of the reactor vessel head. The control rod is also designed to allow uncoupling and coupling from above the vessel using control rod handling tools.

The control rod is positively coupled to the FMCRD and shall be designed to remain coupled during all scrams and loading conditions, including inoperative buffer scram loads. The control rod withstands the loads induced by the FMCRD without exceeding the structural design criteria as stated in sections 4.2.4.1 and 4.2.4.2 above.

The control rod is dimensionally compatible with the fuel assemblies (unirradiated and irradiated). The control rod is guided, rotationally restrained and laterally supported by the adjacent fuel assemblies. The control rod is designed and constructed to establish and maintain the alignment of the control rod drive line (i.e., the control rod, drive housing, CRGT, and fuel assemblies) so that control rod insertion and withdrawal is predictable. The top of the active absorber of a fully withdrawn control rod is below the Bottom of the Active Fuel (BAF). Absorber gap requirements are placed on the control rod in the operating condition to be compatible with the core nuclear design requirements.

4.2.5 Testing, Inspection, and Surveillance Plans

GE has an active program for the surveillance of both production and developmental fuel. The NRC has reviewed the GE program and approved it in Reference 4.2-6.

4.2.6 COL Information

This section contains no requirement for additional information to be provided in support of the combined license. Combined License applicants referencing the ESBWR certified design will address changes to the reference design of the fuel rods, fuel assembly, or control rods from that presented in the DCD.

4.2.7 References

4.2-1 GE Nuclear Energy, “GE Fuel Bundle Designs,” NEDE-31152P, Revision 8, April 2001.

4.2-2 GE Nuclear Energy, “Fuel Rod Thermal Analysis Methodology (GSTRM)”, NEDC-31959P, April 1991.

4.2-3 GE Nuclear Energy, “Cladding Creep Collapse”, NEDC-33139P-A, July 2005.

4.2-4 GE Nuclear Energy, “GE14 for ESBWR Fuel Assembly Mechanical Design Report”, NEDC-33240P, Class III (proprietary), to be issued

4.2-5 GE Nuclear Energy, “GE14 for ESBWR Fuel Rod Thermal-Mechanical Design Report”, NEDC-33242P, Class III (proprietary), to be issued

4.2-6 USNRC Letter, L. S. Rubenstein (NRC) to R. L. Gridley (GE), "Acceptance of GE Proposed Fuel Surveillance Program", June 27, 1984.

4.2-7 GE Nuclear Energy, "GE Marathon Control Rod Assembly," NEDE-31758P-A, October 1991.

4.2-8 GE Nuclear Energy, "ESBWR Marathon Control Rod Mechanical Design Report", NEDC-33244P, Class III (proprietary), to be issued

4.2-9 GE Nuclear Energy, "ESBWR Marathon Control Rod Nuclear Design Report", NEDC-33243P, Class III (proprietary), to be issued

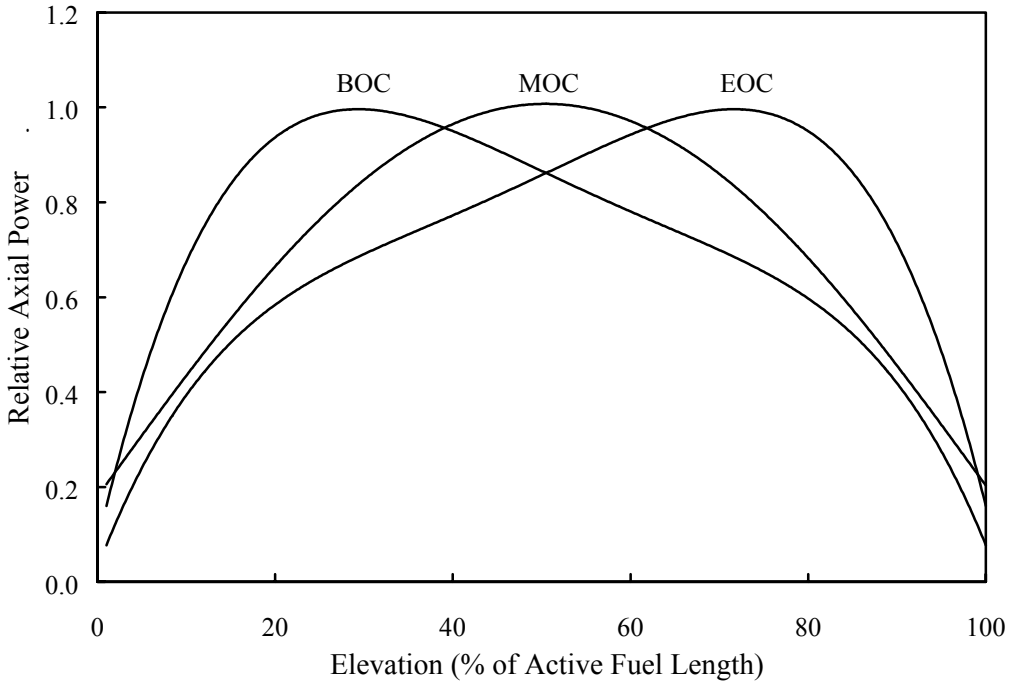

Figure 4.2-1 Axial Power Distributions (Full Length Fuel Rod)

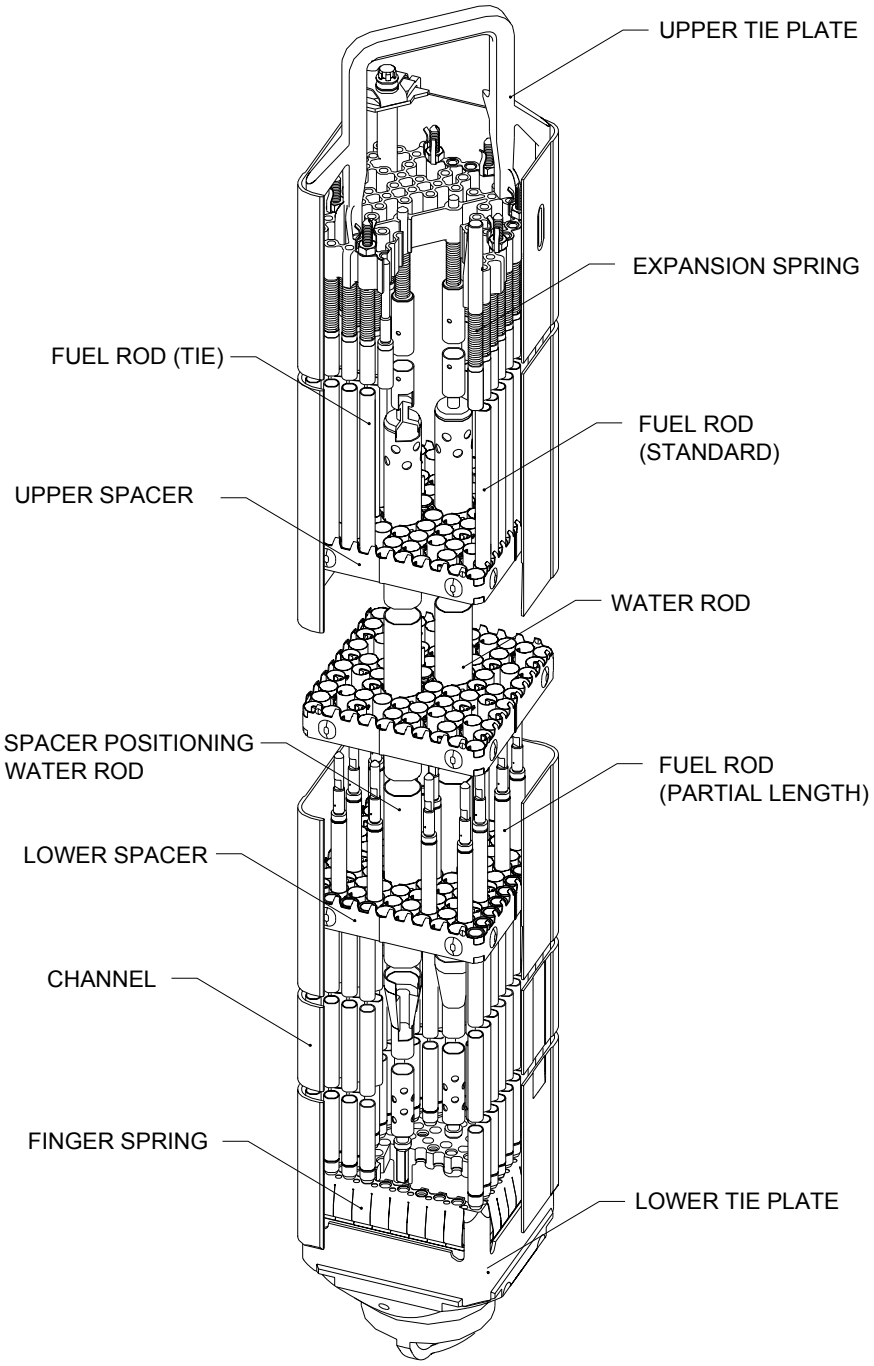

Figure 4.2-2. Typical Fuel Assembly

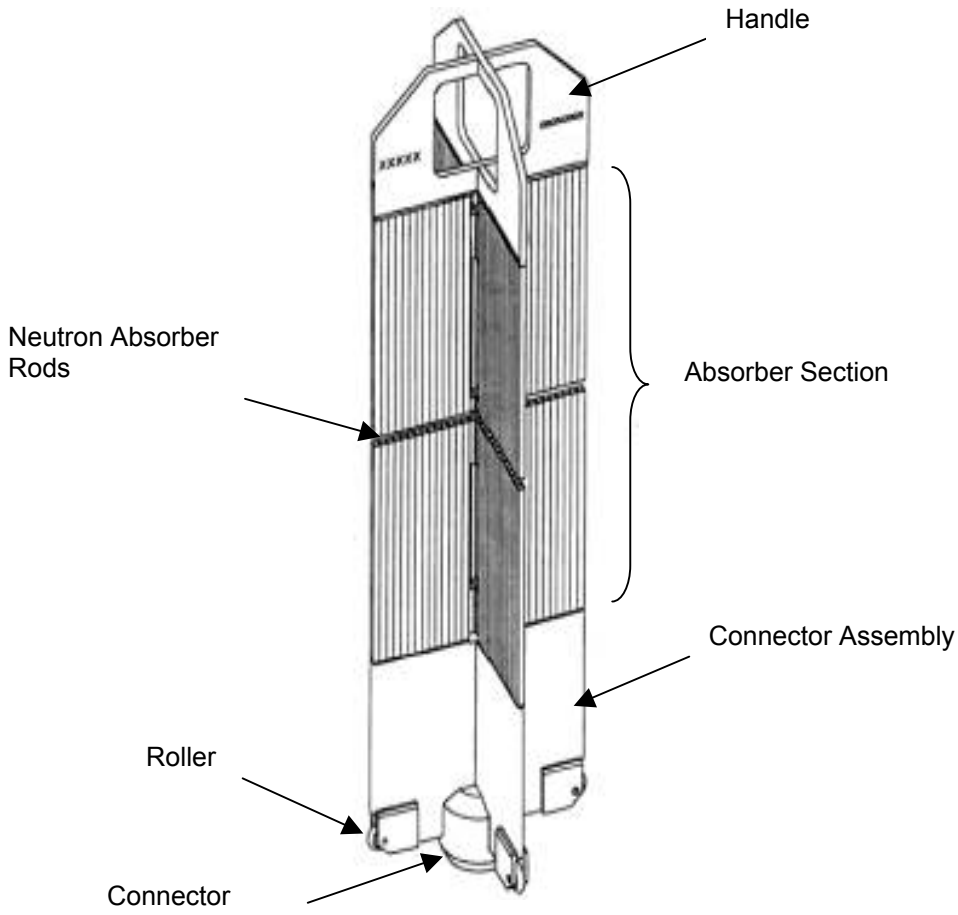

Figure 4.2-3. Typical Control Rod Assembly

‘

Span (except at lower rollers)	= 248.4 +/- 2.3 mm
Maximum Wing Thickness (except as noted on Control Rod Assembly Drawing)	= 9.22 mm
Nominal Absorber Column Length	= 2985 mm

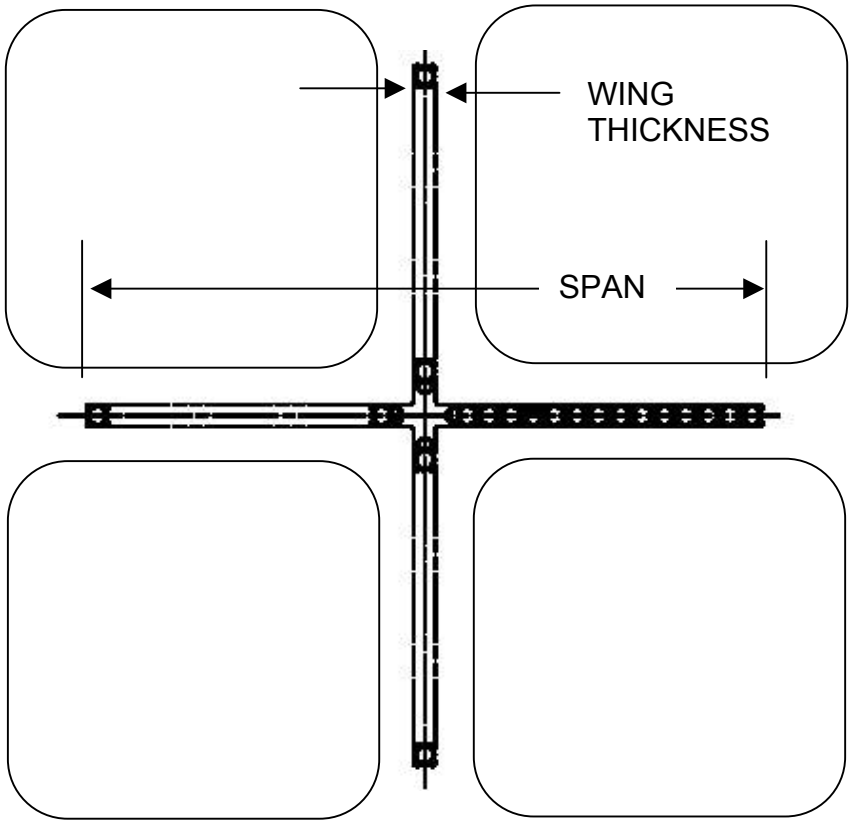

ALL VALUES NOMINAL

Absorber Rods per Wing	= 14
B_4C Density	= 1.76 grams/cm^3
Absorber Tube – Square	= 7.92 mm
Absorber Tube Material	= Stainless Steel
Control Rod Structural Material	= Stainless Steel

Figure 4.2-4. Typical ESBWR Control Rod Configuration

4.3 NUCLEAR DESIGN

This section describes the design bases and functional requirements used in the nuclear design of the fuel, core and reactivity control system and relates these design bases to the General Design Criteria (GDC).

4.3.1 Nuclear Design Bases

The design bases are those that are required for the plant to operate, meeting all safety requirements. The safety design bases that are required fall into two categories:

- The reactivity basis, which prevents an uncontrolled positive reactivity excursion, and
- The overpower bases for the control of power distribution, which prevent the core from operating beyond the fuel integrity limits.

4.3.1.1 Negative Reactivity Feedback Bases

Reactivity coefficients, the differential changes in reactivity produced by differential changes in core conditions, are useful in calculating stability and evaluating the response of the core to external disturbances. The base initial condition of the system and the postulated initiating event determine which of the several defined coefficients are significant in evaluating the response of the reactor. The coefficients of interest are the Doppler coefficient, the moderator void reactivity coefficient and the moderator temperature coefficient. Also associated with the BWR is a power reactivity coefficient. The power coefficient is a combination of the Doppler and void reactivity coefficients in the power operating range; this is not explicitly evaluated. The Doppler coefficient, the moderator void reactivity coefficient and the moderator temperature coefficient of reactivity shall be negative for power operating conditions, thereby providing negative reactivity feedback characteristics.

The above design basis meets General Design Criterion 11.

4.3.1.2 Control Requirements (Shutdown Margins)

The core must be capable of being made subcritical, with margin, in the most reactive condition throughout the operating cycle with the most reactive control rod fully withdrawn and all other rods fully inserted. This satisfies General Design Criterion 26.

4.3.1.3 Control of Power Distribution (Overpower Bases)

The nuclear design basis is that core operation is constrained by the Maximum Linear Heat Generation Rate (MLHGR) and Minimum Critical Power Ratio (MCPR). The MLHGR and the OLMCPR are determined such that, with 95% confidence, the fuel does not exceed required licensing limits during abnormal operational occurrences or accidents.

These parameters are defined as follows:

Maximum Linear Heat Generation Rate: The MLHGR is the maximum linear heat generation rate expressed in kW/ft for the fuel rod with the highest surface heat flux at a given nodal plane in the bundle. The MLHGR operating limit is bundle type dependent. The MLHGR can be monitored to assure that all mechanical design requirements are met. The fuel will not be

operated at MLHGR values greater than those found to be acceptable within the body of the safety analysis under normal operating conditions. Under abnormal conditions, including the maximum overpower condition, the MLHGR will not cause fuel melting, as discussed in Section 4.2.

Minimum Critical Power Ratio: The MCPR is the minimum CPR allowed for a given bundle type to avoid boiling transition. The CPR is a function of several parameters; the most important are bundle power, bundle flow, and bundle R-factor. The R-factor depends on the local power distribution and the details of the bundle mechanical design. The plant Operating Limit MCPR (OLMCPR) is established by considering the limiting anticipated operational occurrences (AOOs) for each operating cycle. The OLMCPR is determined such that 99.9% of the rods avoid boiling transition during the transient of the limiting analyzed AOO, as discussed in Section 4.4.

The above basis satisfies General Design Criterion 10.

4.3.1.4 Stability Bases

The licensing basis for stability must comply with the requirements of 10 CFR 50, Appendix A, "General Design Criteria for Nuclear Power Plants". The Appendix A criteria related to stability are Criteria 10 and 12.

Criterion 10 (Reactor Design) requires that:

> "The reactor core and associated coolant, control, and protection systems shall be designed with appropriate margin to assure that specified acceptable fuel design limits are not exceeded during any condition of normal operation, including the effects of anticipated operational occurrences."

Criterion 12 (Suppression of Reactor Power Oscillations) requires that:

> "The reactor core and associated coolant, control, and protection systems shall be designed to assure that power oscillations which can result in conditions exceeding specified acceptable fuel design limits are not possible or can be reliably and readily detected and suppressed."

4.3.2 Nuclear Design Analytical Methods

4.3.2.1 Steady-state nuclear methods

The principal tool used in the steady-state nuclear core analysis is the three-dimensional BWR simulator code, which computes core reactivity, power distributions, exposure, and reactor thermal-hydraulic characteristics, with spatially varying voids, control rods, burnable poisons and other variables. It is used to calculate reactivity variations through the cycle, shutdown margins and thermal limits (MLHGR and MCPR).

The steady-state nuclear evaluations of the reference core design are performed using the analytical tools and methods approved in Reference 4.3-2. The applicability of these methods to the nuclear analysis of ESBWR is given in Reference 4.3-8. Changes may be made to these techniques provided that NRC-approved methods, models, and application methodologies are used.

Neutronic parameters used by core simulator are obtained from the 2-D lattice physics code and parametrically fitted as a function of moderator density, exposure, control and moderator density history for a given fuel type. Lattice physics calculations are performed using a two-dimensional, fine mesh, few group diffusion theory computer program (TGBLA) that determines the nodal flux and power distributions in a fuel bundle (Reference 4.3-2). The lattice analyses are performed during the bundle design process. The results of these single bundle calculations are reduced to "libraries" of lattice reactivities, relative rod powers, and few group cross-sections as a function of instantaneous void, exposure, exposure-void history, control state and history, and fuel and moderator temperature. The lattice analyses depend only on fuel lattice parameters and are valid for all plants and cycles for a specific bundle design. The ESBWR core is of the N-lattice type, which is identical to the ABWR, and the lattice physics methods have been qualified for this geometry, including core tracking of operating ABWRs.

This program calculates lattice average nuclear constants, rod-by-rod distribution of power and lattice average isotopic data for an infinite array of identical lattices. These are all calculated as a function of exposure, voids, control state, and temperature. Specific applications include fuel lattice design, fuel bundle design and fuel bundle reconstitution physics analysis.

The solution technique begins with the generation of thermal broad-group neutron cross sections for all homogenized fuel rod cells and external regions in a bundle. In the thermal energy range, the rod-by-rod thermal spectra are calculated by a collision probability method similar to the THERMOS formulation. The major difference is that neutron leakage from rod to rod is taken into account. The leakage is determined by diffusion theory and is fed into the thermal spectrum calculation. Iterations between diffusion theory and thermal spectrum calculations are carried out to determine accurate, spatially dependent, thermal cross sections. In the epithermal and fast energy range, the level-wise resonance integrals are calculated by an improved intermediate resonance (IR) approximation in which the IR parameters are fuel-rod-temperature dependent. The fast and epi-thermal regional flux is determined by a multi-group collision probability process.

A two-dimensional, coarse-mesh, broad-group, diffusion-theory calculation is used to determine the nodal flux distributions in the bundle. By combining the two-dimensional, coarse-mesh, broad-group flux and the intra-nodal collision probability flux profiles, the lattice intra-nodal flux and power distributions are obtained. In the depletion calculation, 100 nuclides are treated, including 25 fissile and fertile nuclides and up to 48 fission products, one pseudo fission product and one gadolinia tail pseudo product. A Runga-Kutta-Gill burnup integration scheme is employed to determine the isotopic inventory for fuel material depletion. TGBLA includes a sub-channel void distribution model to capture the impact of non-uniform voids on local pin powers.

The BWR core simulator (PANACEA) is a static, three-dimensional coupled nuclear-thermal-hydraulic computer program representing the BWR core exclusive of any external flow loops. Provisions are made for fuel cycle and thermal limits calculations. The program is used for detailed three-dimensional design and operational calculations of BWR neutron flux and power distributions and thermal performance as a function of control rod position, refueling pattern, coolant flow, reactor pressure, and other operational and design variables. A power-exposure iteration option is available for target exposure distribution and cycle length predictions.

The nuclear model is based on coarse-mesh nodal, static diffusion theory. Eigenvalue iteration yields the fundamental mode solution. This is coupled to static parallel channel thermal-hydraulics containing a modified Zuber-Findlay void-quality correlation. Pressure drop balancing yields the flow distribution among the channels.

These methods (TGBLA06/PANAC11) include a 1½ energy group neutron diffusion model with non-linearly coupled spatially asymptotic thermal flux model, spectral history reactivity model, control blade history reactivity and local peaking models, explicit temperature (density) dependence for cold critical data, pin power reconstruction, and internal cross section library generation. The control blade history model uses TGBLA cross section data from a controlled depletion with uncontrolled restarts for each specific fuel type. The impacts on reactivity and local peaking are included using an exponentially weighted scheme.

PANACEA is used in core design and operational calculations to produce reactivity, power distribution, and thermal performance information as functions of design and operational variables such as fuel loading pattern, control rod position, coolant flow, and reactor pressure. Specific applications include fuel loading, fuel cycles, core design configuration, core management and on site core monitoring.

TRACG is iteratively used with the simulator code to establish the total core flow for a given core power in order to account for the flow loop external to the core. This iteration is described in Section 4.4. The application of TRACG to the ESBWR core is described in Reference 4.3-7. The ESBWR core is not substantially different from operating BWRs from the viewpoint of steady-state nuclear simulations of core parameters.

4.3.2.2 Reactivity Coefficient Methods

The Doppler reactivity coefficient is determined by using an NRC-approved lattice physics code. The Doppler coefficient is determined using the theory and methods for steady-state nuclear calculations, described above.

The lattice physics code is used to calculate k∞ for any lattice at two temperatures. The first temperature is the standard hot operating temperature. The second temperature is set at 1773 K. The calculations are made at as a function of void fraction and at every standard hot uncontrolled exposure depletion point.

The Doppler Reactivity Coefficient (DRC) is characterized as follows:

$$DRC = \frac{1000(k_{T_1} - k_{T_0})}{k_{T_0}\left(\sqrt{T_1} - \sqrt{T_0}\right)}$$

where:

T_0 = normal hot operating temperature (Kelvin).

T_1= elevated temperature (Kelvin).

k_{T1} = eigenvalue at elevated temperature.

k_{T0}= eigenvalue at normal operating temperature.

While the reactivity change caused by the Doppler effect is small compared to the moderator

void reactivity changes during normal operation, it becomes very important during postulated rapid power excursions in which large fuel temperature changes occur (see Chapter 15).

The 3D core simulator is used in determining the void coefficient of reactivity. A detailed discussion of the methods used to calculate moderator void reactivity coefficients, the accuracy and application to plant transient analyses, is presented in Reference 4.3-4. The In-Channel Void Coefficient (VODCOF) is the ratio of the change in k-effective to the change in (percent) void fraction because of a perturbation in some particular parameter:

$$VODCOF = \frac{1}{k}\frac{\partial k}{\partial(\%VOID)}$$

The calculation of the void reactivity coefficient is accomplished through perturbation of the inlet enthalpy to the core, although perturbation of pressure or core flow are also possible to effect a change in voids and reactivity. The derivative in the above equation is determined by a higher-order numerical scheme, which requires two points above and two points below the base point in addition to the base point itself. After evaluating four perturbations to the original system, one obtains a better estimate than any of the original four approximate derivatives. This type of evaluation is subsequently less sensitive to the type and size of the perturbation for evaluation of a particular derivative.

The moderator temperature coefficient (MODCOF) is calculated using a combination of the lattice physics code and core simulator. The lattice physics code is used to evaluate infinite lattice properties of each of the various lattices in the fuel bundle as a function of exposure, void history and temperature. Introducing the temperature specific nuclear libraries from the lattice physics code into the core simulator and performing a standard cold eigenvalue calculation then simulate a core temperature change. From the differential in core eigenvalue, the moderator temperature coefficient of reactivity may be obtained as:

$$MODCOF = \frac{1}{k}\frac{\partial k}{\partial(^{\circ}K)}$$

4.3.2.3 Stability Methods

A detailed discussion of the methods used to analyze ESBWR thermal hydraulic stability is presented in Reference 4.3-7.

4.3.3 Nuclear Design Evaluation

The core design consists of a light-water moderated reactor, fueled with slightly enriched uranium-dioxide. The use of water as a moderator produces a neutron energy spectrum in which fissions are caused principally by thermal neutrons. At normal operating conditions, the moderator boils, producing a spatially variable distribution of steam voids in the core. The void reactivity feedback effect is an inherent safety feature of the ESBWR system. Any system change which increases reactor power, either in a local or core-wide sense, produces additional steam voids and thus reduces the power.

4.3.3.1 Nuclear Design Description

The reference core design is examined in detail in Reference 4.3-8. The reference core design is characterized by the loading pattern given in Figure 4.3-1. This core design is the basis for the system analyses in other sections of this Design Control Document. For cores other than the reference core design or the initial core, the Reference Loading Pattern (RLP) is the nuclear design basis for fuel licensing. The RLP core is designed to represent, as closely as possible, the actual core loading pattern. However, there may be occurrences where the number and/or types of bundles in the reference design and the actual core loading do not exactly agree. Any differences between the reference loading pattern and the actual loading pattern are evaluated to ensure that there is no adverse impact to key parameters that may affect the licensing calculations.

4.3.3.2 Negative Reactivity Feedback Evaluation

Reactivity coefficients are a measure of the differential changes in reactivity produced by differential changes in core conditions. These coefficients are useful in understanding the response of the core to external disturbances. The Doppler reactivity coefficient and the moderator void reactivity coefficient are the two primary reactivity coefficients that characterize the dynamic behavior of boiling water reactors.

The safety analysis methods (described in Chapter 15) are based on system and core models that include an explicit representation of the core space-time kinetics. Therefore, the reactivity coefficients are not directly used in the safety analysis methods, but are useful in the general understanding and discussion of the core response to perturbations.

4.3.3.2.1 Doppler Reactivity Coefficient Evaluation

The Doppler coefficient is a measure of the reactivity change associated with an increase in the absorption of resonance-energy neutrons caused by a change in the temperature of the material in question. The Doppler reactivity coefficient provides instantaneous negative reactivity feedback to any rise in fuel temperature, on either a gross or local basis. The magnitude of the Doppler coefficient is inherent in the fuel design and does not vary significantly among BWR designs. For most structural and moderator materials, resonance absorption is not significant, but in U-238 and Pu-240 an increase in temperature produces a comparatively large increase in the effective absorption cross-section. The resulting parasitic absorption of neutrons causes an immediate loss in reactivity.

Analyses were performed using the analytical models described above, as described in Reference 4.3-8. The values are identical to the analysis supporting compliance for GE14 found in Reference 4.3-3, which consist of examination of the lattice level Doppler coefficients for several lattice configurations. Evaluating the Doppler coefficient at the 2D lattice level obviates the need for more detailed calculations involving the 3D core simulator. For all cases evaluated, the calculated Doppler coefficient was found to be negative. A typical value calculated is $-1.10\ \Delta k/°K^{0.5}$ (at zero exposure, 0.4 void fraction).

4.3.3.2.2 Moderator Void Coefficient Evaluation

The moderator void coefficient should be large enough to prevent power oscillation due to spatial xenon changes yet small enough that pressurization transients do not unduly limit plant

operation. In addition, the void coefficient has the ability to flatten the radial power distribution and to provide ease of reactor control due to the void feedback mechanism. The overall void coefficient is always negative over the complete operating range.

Analyses of the moderator void coefficient of the reference core design were performed, as described in Reference 4.3-8. The results of these analyses show that boiling of the moderator in the active channel flow area results in negative reactivity feedback for all expected modes of operation. The operating mode selected to represent the most limiting condition (the least negative value of moderator void coefficient) was the cold critical state at the middle of an equilibrium cycle. The value of moderator void coefficient for this condition was calculated to be -0.0052 Δk/% void at zero void, for a moderator temperature of 100 °C at the middle of the reference design fuel cycle. The variation of the void coefficient as a function of temperature is shown in Figure 4.3-2 for several exposure points in the reference fuel cycle.

4.3.3.2.3 Moderator Temperature Coefficient Evaluation

The moderator temperature coefficient is associated with the change in the water moderating capability. A negative moderator temperature coefficient during power operation provides inherent protection against power excursions. Hot standby is the condition under which the BWR core coolant has reached rated pressure and the temperature at which boiling has begun. Once boiling begins, the moderator temperature remains essentially constant in the boiling regions.

Analyses of the moderator temperature coefficient of the reference core design were performed, as described in Reference 4.3-8. The variation of the moderator temperature coefficient as a function of temperature is shown in Figure 4.3-3 for several exposure points in the reference fuel cycle.

The most limiting state condition was determined to be at the end of the reference fuel cycle for a critical core configuration. The results of the analyses at these conditions were that the moderator temperature coefficient is negative for all moderator temperatures above approximately 115°C. At hot standby conditions, the moderator temperature ranges from approximately 260°C at the core inlet to approximately 288°C in the boiling regions of the core. Therefore, the moderator temperature coefficient criteria are met with considerable margin.

The results of these analyses at these conditions indicate that the moderator temperature coefficient is negative for all moderator temperatures in the operating temperature range. Therefore, the moderator temperature coefficient criteria are met.

4.3.3.3 Control Requirements Evaluation

The ESBWR control rod system is designed to provide adequate shutdown margin and control of the maximum excess reactivity anticipated during the plant operation.

4.3.3.3.1 Shutdown Margin Evaluation

The shutdown margin is determined by using the BWR simulator code to calculate the core multiplication at selected exposure points with the strongest rod fully withdrawn. The minimum required shutdown margin is given in the technical specifications.

As exposure accumulates and burnable poison depletes in the lower exposure fuel bundles, an increase in core reactivity may occur. The nature of the increase depends on specifics of fuel loading and control state. For fuel cycles beyond the initial core, the shutdown margin is calculated based on the carryover of the expected exposure at the end of the previous cycle. The core is assumed to be in the cold, xenon-free condition in order to ensure that the calculated values are conservative. Further discussion of the uncertainty of these calculations is given in Reference 4.3-5.

The cold k_{eff} is calculated with the strongest control rod out at various exposures through the cycle. A value R is defined as the difference between the strongest rod out k_{eff} at beginning of cycle (BOC) and the maximum calculated strongest rod out k_{eff} at any exposure point.

The strongest rod out k_{eff} at any exposure point in the cycle is equal to or less than

$$k_{eff} = k_{eff}(\textit{Strongest rod withdrawn @ BOC}) + R.$$

Where R is always greater than or equal to 0. The value of R includes equilibrium Sm.

The calculated k_{eff} with the strongest rod withdrawn at BOC are reported in Table 4.3-1. The uncontrolled and fully controlled k_{eff} values are also reported in Table 4.3-1. The minimum required shutdown margin is given in the technical specifications. Details of the calculation of shutdown margin are given in Reference 4.3-8.

4.3.3.3.2 Reactivity Variation Evaluation

The excess reactivity designed into the core is controlled by the control rod system supplemented by gadolinia-urania fuel rods. These integral fuel burnable absorber rods may be used to provide partial control of the excess reactivity available during the fuel cycle. In doing so, the burnable absorber loading controls peaking factors and prevents the moderator temperature coefficient from being positive at normal operating conditions. The burnable absorber performs this function by reducing the requirement for control rod inventory in the core at the beginning of the fuel cycle, as described previously. Control rods are used during the cycle to compensate for reactivity changes due to burnup and also to control the power distribution.

The nuclear design of the fuel assemblies comprising the equilibrium cycle reference core design, including enrichment and burnable absorber distributions within the assembly, is given in Reference 4.3-8, as is information relating to the reactivity variation through the cycle (i.e., hot excess reactivity). The control rod patterns through the cycle of the reference core design are given in Appendix 4A using a quarter core (mirror reflected) representation.

4.3.3.3.3 Standby Liquid Control System Evaluation

The Standby Liquid Control System (SLCS) is designed to provide the capability of bringing the reactor, at any time in a cycle, from full power with a minimum control rod inventory (which is defined to be at the peak of the xenon transient) to a subcritical condition with the reactor in the most reactive xenon-free state. The SLCS is described in detail in Subsection 9.3.5.

The requirements of this system are dependent primarily on the reactor power level and on the reactivity effects of voids and temperature between full-power and cold, xenon-free conditions. The shutdown capability of the SLCS for the reference ESBWR core is demonstrated in Reference 4.3-8. The shutdown margin is calculated for a uniformly mixed equivalent

concentration of natural boron, which is required in the reactor core to provide adequate cold shutdown margin after operation of the SLCS.

4.3.3.4 Criticality of Reactor During Refueling Evaluation

The basis for maintaining the reactor subcritical during refueling is presented in Subsection 4.3.1.2, and a discussion of how control requirements are met is given in Subsection 4.3.3.3.1. The minimum required shutdown margin is given in the technical specifications.

4.3.3.5 Power Distribution Evaluation

The core power distribution is a function of fuel bundle design, core loading, control rod pattern, core exposure distributions and core coolant flow rate. The thermal performance parameters, MLHGR and MCPR, limit the core power distribution. The analysis of the performance of the reference core design in terms of power distribution, and the associated MLHGR and MCPR distributions within the core throughout the cycle exposure, is given in detail in Reference 4.3-8.

4.3.3.5.1 Power Distribution Measurements

The techniques for measurement of the power distribution within the reactor core, together with instrumentation correlations and operation limits, are discussed in Subsection 7A.3.2.

4.3.3.5.2 Power Distribution Accuracy

The accuracy of the calculated power distribution is discussed in Reference 4.3-1.

4.3.3.5.3 Power Distribution Anomalies

Stringent inspection procedures are utilized to ensure the correct arrangement of the core following fuel loading. A fuel loading error (a mislocated or a misoriented fuel bundle in the core) is a very improbable event, but calculations have been performed to determine the effects of such events. The fuel loading error is discussed further in Chapter 15.

The inherent design characteristics of the ESBWR are well suited to limit gross power tilting. The stabilizing nature of the large moderator void coefficient effectively reduces the effect of perturbations on the power distribution. In addition, the in-core instrumentation system, together with the online computer, provides the operator with prompt information on the power distribution so that control rods or other means to limit the undesirable effects of power tilting can readily be used. Because of these design characteristics, it is not necessary to allocate a specific margin in the peaking factor to account for power tilt. If, for some reason, the power distribution cannot be maintained within normal limits using control rods, then the total core power can be reduced.

4.3.3.6 Stability Evaluation

4.3.3.6.1 Xenon Transients

Boiling water reactors do not have instability problems due to xenon. This has been demonstrated by:

- Never having observed xenon instabilities in operating BWRs;

- Special tests which have been conducted on operating BWRs in an attempt to force the reactor into xenon instability; and
- Calculations.

All of these indicators have proven that xenon transients are highly damped in a BWR due to the large negative moderator void feedback. Xenon stability analysis and experiments are reported in Reference 4.3-6. Specific evaluations demonstrating the damping of xenon transients (oscillations) in the ESBWR core are carried out in Reference 4.3-8.

4.3.3.6.2 Thermal Hydraulic Stability

The ESBWR licensing basis for stability satisfies GDC 12 by designing the reactor system such that significant power oscillations are not possible. A high degree of confidence is established that oscillations will not occur by imposing conservative design criteria on the channel, core wide and regional decay ratios under all conditions of normal operation and anticipated transients.

Because oscillations in power and flow are precluded by design, the requirements of GDC 10 are met through the analysis for AOOs, and are automatically satisfied with respect to stability.

In addition, the ESBWR will implement a Detect and Suppress solution as a defense-in-depth system. The thermal hydraulic stability is discussed in detail in Appendix 4D.

4.3.4 Changes

Not applicable.

4.3.5 COL Information

This section contains no requirement for additional information to be provided in support of the combined license. Combined License applicants referencing the ESBWR certified design will address changes to the reference design of the fuel or core design from that presented in the DCD.

4.3.6 References

4.3-1 Letter from R. J. Reda (GE) to R. C. Jones (NRC), MFN-098-96, "Implementation of Improved GE Steady-State Methods", July 2, 1996.

4.3-2 Letter from Stuart A. Richards to Glen A. Watford, “Amendment 26 to GE Licensing Topical Report NEDE–24011–P–A, GESTAR II – Implementing Improved GE Steady–State Methods (TAC No. MA6481),” November 10, 1999.

4.3-3 Global Nuclear Fuel, “GE14 Compliance With Amendment 22 of NEDE-24011-P-A (GESTAR II),” NEDC-32868P, Rev. 1, September 2000.

4.3-4 R. C. Stirn, “Generation of Void and Doppler Reactivity Feedback for Application to BWR Design,” NEDO–20964, December 1975.

4.3-5 General Electric Company, “BWR/4,5,6 Standard Safety Analysis Report,” Revision 2, Chapter 4, June 1977.

4.3-6 R. L. Crowther, "Xenon Considerations in Design of Boiling Water Reactors," APED–5640, June 1968.

4.3-7 General Electric Company, "TRACG Application for ESBWR Stability Analysis," NEDE-33083, Supplement 1, B. S. Shiralkar, et al., December 2004.

4.3-8 Global Nuclear Fuel, "GE14 for ESBWR Nuclear Design Report", NEDC-33239P, to be issued.

Table 4.3-1

Calculated Core Effective Multiplication and Control System Worth - No Voids, 20°C

Control Rod Pattern *	K-effective
Uncontrolled	1.1112
Fully Controlled	0.9508
Strongest Control Rod Out	0.9843

* For the Reference Core Loading Pattern at the limiting exposure of 0 GWd/MT.

	1	2	3	4	5	6	7	8	9	10	11	12	13	14	15	16	17	18	19	
1															33.4	32.3	35.3	32.6	33.8	76
2													39.0	34.1	33.3	17.4	16.0	15.3	0.0	74
3											35.7	33.4	17.9	0.0	19.6	20.5	18.0	0.0	30.5	72
4									35.6	33.7	16.1	0.0	0.0	0.0	20.5	18.6	0.0	0.0	13.4	70
5								37.3	13.5	0.0	0.0	0.0	17.0	0.0	0.0	0.0	29.4	0.0	20.5	68
6							34.7	14.8	0.0	0.0	0.0	19.4	0.0	20.7	0.0	21.1	0.0	20.9	0.0	66
7						34.7	35.3	0.0	16.7	0.0	29.2	18.2	0.0	0.0	24.7	18.9	20.0	0.0	21.4	64
8					37.3	14.8	0.0	0.0	0.0	20.1	15.7	28.6	0.0	12.2	14.0	14.6	0.0	19.9	20.9	62
9				35.6	13.5	0.0	16.7	0.0	16.9	0.0	0.0	0.0	19.1	0.0	19.9	0.0	20.0	0.0	19.9	60
10				33.7	0.0	0.0	0.0	20.1	0.0	21.0	0.0	19.8	0.0	20.5	0.0	0.0	0.0	20.0	0.0	58
11			35.8	16.1	0.0	0.0	29.2	15.7	0.0	0.0	27.8	19.9	19.7	0.0	28.0	19.9	20.3	0.0	21.2	56
12			33.4	0.0	0.0	19.4	18.2	28.6	0.0	19.8	19.9	20.8	0.0	0.0	19.8	20.3	0.0	0.0	20.1	54
13		39.0	17.9	0.0	16.9	0.0	0.0	0.0	19.1	0.0	19.7	0.0	21.0	0.0	20.1	0.0	20.5	0.0	20.4	52
14		34.1	0.0	0.0	0.0	20.7	0.0	12.2	0.0	20.5	0.0	0.0	0.0	20.8	0.0	20.1	0.0	20.0	0.0	50
15	33.4	33.3	19.6	20.5	0.0	0.0	24.7	14.0	19.9	0.0	28.0	19.8	20.1	0.0	27.8	20.7	0.0	0.0	26.4	48
16	32.3	17.4	20.5	18.6	0.0	21.1	18.9	14.6	0.0	0.0	19.9	20.3	0.0	20.1	20.6	20.8	0.0	19.5	20.6	46
17	35.3	16.0	18.0	0.0	29.4	0.0	19.9	0.0	20.0	0.0	20.3	0.0	20.5	0.0	0.0	0.0	20.9	0.0	20.5	44
18	32.6	15.3	0.0	0.0	0.0	20.8	0.0	19.9	0.0	20.0	0.0	0.0	0.0	20.0	0.0	19.5	0.0	21.0	0.0	42
19	33.8	0.0	30.5	13.4	20.5	0.0	21.4	20.9	19.9	0.0	21.2	20.1	20.4	0.0	26.4	20.6	20.5	0.0	21.0	40
	1	3	5	7	9	11	13	15	17	19	21	23	25	27	29	31	33	35	37	

Figure 4.3-1. Core Loading Map – Reference Loading Pattern Exposures (GWD/ST)

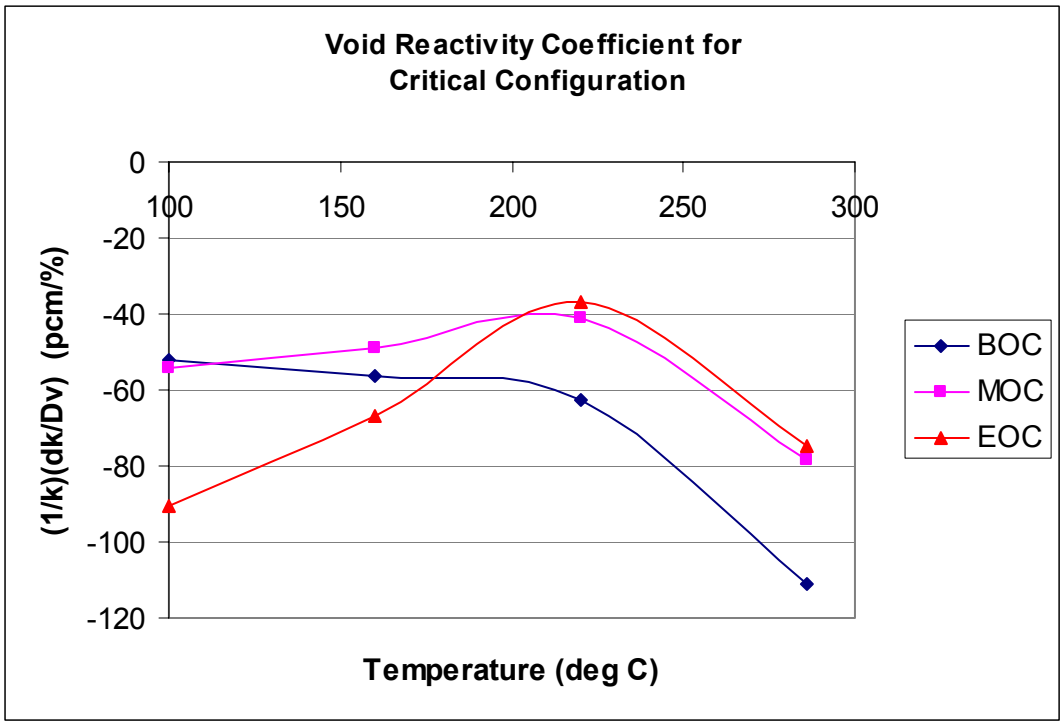

Figure 4.3-2. Moderator Void Coefficient for Reference Core Design

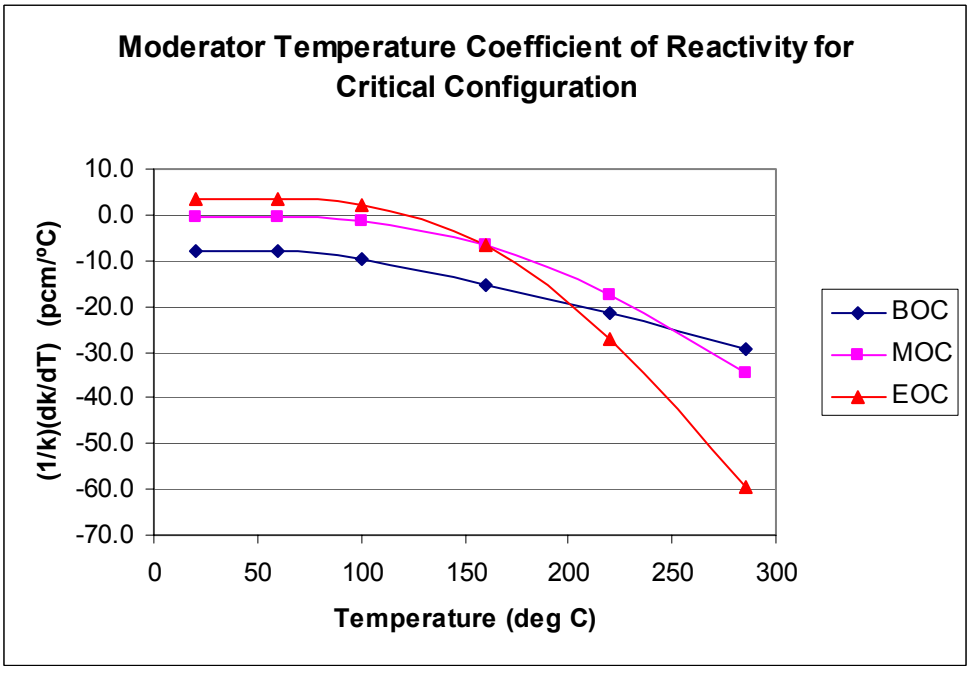

Figure 4.3-3. Moderator Temperature Coefficient for Reference Core Design

4.4 THERMAL AND HYDRAULIC DESIGN

This section describes the design bases and functional requirements used in the thermal and hydraulic design of the fuel, core and reactivity control system and relates these design bases to the General Design Criteria (GDC).

4.4.1 Reactor Core Thermal and Hydraulic Design Basis

Thermal-hydraulic design of the core shall establish the thermal-hydraulic safety limits for use in evaluating the safety margin in accordance with GDC 10.

Margin to specified acceptable fuel design limits is maintained during normal steady-state operation when the minimum critical power ratio (MCPR) is greater than the required MCPR operating limit (OLMCPR) and the linear heat generation rates (LHGRs) is maintained below the maximum LHGR (MLHGR) limit(s). The steady-state OLMCPR and MLHGR limits are determined by analysis of the most severe anticipated operational occurrences (AOOs) to accommodate uncertainties and provide reasonable assurance that no fuel damage results during AOOs. The Technical Specifications require these limits.

4.4.1.1 Critical Power Ratio Bases

The objective for normal operation and AOOs is to maintain nucleate boiling and thus avoid a transition to film boiling. Limits are specified to maintain adequate margin to the onset of the boiling transition. The figure of merit utilized for plant operation is the critical power ratio (CPR). The CPR is the ratio of the bundle power at which some point within the assembly experiences onset of boiling transition to the operating bundle power. Thermal margin is stated in terms of the minimum value of the critical power ratio (MCPR) that corresponds to the most limiting fuel assembly in the core. The design requirement is based on a statistical analysis such that for AOOs at least 99.9% of the fuel rods would be expected to avoid boiling transition (Reference 4.4-8 and 4.4-9).

4.4.1.1.1 Fuel Cladding Integrity Safety Limit Bases

GDC 10 requires, and safety limits ensure, that specified acceptable fuel design limits are not exceeded during steady state operation, normal operational transients, and anticipated operational occurrences (AOOs). Since the parameters that result in fuel damage are not directly observable during reactor operation, the thermal and hydraulic conditions that result in the onset of transition boiling have been used to mark the beginning of the region in which fuel damage could occur. The Fuel Cladding Integrity Safety Limit (FCISL) is set such that no significant fuel damage is calculated to occur during normal operation and AOOs. Although it is recognized that the onset of transition boiling would not result in damage to BWR fuel rods, a calculated fraction of rods expected to avoid boiling transition has been adopted as a convenient limit. The FCISL is defined as the fraction (%) of total fueled rods that are expected to avoid boiling transition during normal operation and AOOs. A value of 99.9% provides assurance that specified acceptable fuel design limits are met.

4.4.1.1.2 MCPR Operating Limit Calculation Bases

A plant-unique MCPR operating limit is established to provide adequate assurance that the FCISL for that plant is not exceeded for any AOO. This operating requirement is obtained by statistically combining the maximum ΔCPR/ICPR (delta CPR divided by the initial CPR) value for the most limiting AOO from conditions postulated to occur at the plant with the uncertainties associated with plant initial conditions and modeling of the transient ΔCPR.

4.4.1.2 Void Fraction Distribution Bases

The void fraction in a boiling water reactor (BWR) fuel bundle has a strong effect on the nuclear flux and power distribution. Therefore accurate prediction of the void fraction is important for evaluation of the performance of the BWR reactor and fuel. In design and licensing calculations the void fraction is evaluated using empirical correlations based on the characteristic dimensions of the fuel bundle and hydraulic properties of the two-phase flow in the fuel bundle.

4.4.1.3 Core Pressure Drop and Hydraulic Loads Bases

The accuracy on the prediction of core pressure drop is essential to the modeling of fuel and core inlet flow and hydraulic loads.

4.4.1.4 Core Coolant Flow Distribution Bases

Based on the prediction of core pressure drop, the distribution of flow into the fuel channels and the core bypass regions are calculated. The core coolant flow distribution forms the basis of the prediction of steady state and transient critical power and void fraction.

4.4.1.5 Fuel Heat Transfer Bases

The model must accurately predict heat transfer between the coolant, fuel rod surface, cladding, gap, and fuel pellet in the evaluation of core and fuel safety criteria.

4.4.1.6 Maximum Linear Heat Generation Rate Bases

The Maximum Linear Heat Generation Rate (MLHGR) bases are described in Section 4.2. The adequacy of MLHGR limits are evaluated for the most severe anticipated operational occurrences (AOOs) to provide reasonable assurance that no fuel damage results during AOOs.

4.4.1.7 Summary of Design Bases

The steady-state operating limits have been established to assure that the design bases are satisfied for the most severe AOO. Demonstration that the steady-state MCPR and MLHGR limits are not exceeded is sufficient to conclude that the design bases are satisfied.

4.4.2 Reactor Core Thermal and Hydraulic Methods

This section contains a description of the application of NRC-approved methods to the ESBWR. Changes may be made to these techniques provided that NRC-approved (including applicability to ESBWR) methods, models, and application methodologies are used.

4.4.2.1 Critical Power Methods

The qualification of the critical power methods for ESBWR is discussed in Section 4.4.3.

4.4.2.1.1 Bundle Critical Power Performance Method

Bundle critical power performance methodology is described in Reference 4.4-8.

4.4.2.1.2 Fuel Cladding Integrity Safety Limit Statistical Method

The statistical analysis utilizes a model of the core that simulates the process computer function. The code produces a critical power ratio (CPR) map of the core based on steady state uncertainties defined by Reference 4.4-8 and 4.4-13. This is coupled with the TRACG ΔCPR/ICPR results to determine the OLMCPR. Details of the procedure are documented in Appendix IV of Reference 4.4-8 and Section 4.6.3 of Reference 4.4-9. Random Monte Carlo selections of all operating parameters based on the uncertainty ranges of manufacturing tolerances, uncertainties in measurement of core operating parameters, calculation uncertainties, the uncertainty in the calculation of the transient ΔCPR/ICPR and statistical uncertainty associated with the critical power correlations are imposed on the analytical representation of the core and the resulting bundle critical power ratios are calculated.

The minimum allowable operating critical power ratio (OLMCPR) is set to correspond to the FCISL (99.9% of the rods are expected to avoid boiling transition) by interpolation among the means of the distributions formed by all the trials.

4.4.2.1.3 MCPR Operating Limit Calculation Method

All ESBWR AOO events are analyzed using the TRACG model described in Reference 4.4-10. The core thermal hydraulic models have been qualified in 4.4-11. Uncertainties have been developed for all High and Medium ranked model parameters. The model uncertainties are documented in Reference 4.4-9. The ΔCPR/ICPR is calculated in accordance with Reference 4.4-9.

4.4.2.2 Void Fraction Methods

The TRACG void fraction model is described in Reference 4.4-10. The model utilized in the core design analysis is described in Reference 4.4-6. Details on the qualification of the TRACG model is contained in Reference 4.4-11. Details on the qualification of the core simulator model void fraction are contained in Attachment A to Reference 4.4-13.

4.4.2.3 Core Pressure Drop and Hydraulic Loads Methods

The TRACG methods for core pressure drop modeling are described in Reference 4.4-10. The TRACG hydraulic formulation for core pressure drop is identical to the model utilized in the core design analysis with the exception of the acceleration pressure drop component. The models utilized in the core design analysis are as follows:

4.4.2.3.1 Friction Pressure Drop

Friction pressure drop is calculated with a basic model as follows:

$$\Delta P_f = \frac{w^2}{2 g_c \rho} \frac{fL}{D_H A_{ch}^2} \phi_{TPF}^2$$

where

ΔP_f = friction pressure drop, psi

w = mass flow rate

g_c = conversion factor

ρ = average nodal liquid density

D_H = channel hydraulic diameter

A_{ch} = channel flow area

L = incremental length

f = friction factor

ϕ_{TPF} = two–phase friction multiplier

The formulation for the two-phase multiplier is similar to that presented in References 4.4-4 and 4.4-5, and is based on data from prototypical BWR fuel bundles.

4.4.2.3.2 Local Pressure Drop

The local pressure drop is defined as the irreversible pressure loss associated with an area change, such as the orifice, lower tie plate, and spacers of a fuel assembly.

The general local pressure drop model is similar to the friction pressure drop and is

$$\Delta P_L = \frac{w^2}{2 g_c \rho} \frac{K}{A_{ch}^2} \phi_{TPL}^2$$

where

ΔP_L = local pressure drop, psi

K = local pressure drop loss coefficient

A = reference area for local loss coefficient

ϕ_{TPL} = two–phase local multiplier

and w, g_c, and ρ are as previously defined. The formulation for the two-phase multiplier is similar to that reported in Reference 4.4-5. Empirical constants were added to fit the results to data taken for the specific designs of the BWR fuel assembly. These data were obtained from tests performed in single-phase water to calibrate the orifice, the lower tie plate, and the holes in the lower tie plate, and in both single and two-phase flow, to derive the best fit design values for spacer and upper tie plate pressure drop. The range of test variables was specified to include the

range of interest for boiling water reactors. New test data are obtained whenever there is a significant design change to ensure the most applicable methods are used. The data applicable to ESBWR is discussed in Section 4.4.2.6.2.5.

4.4.2.3.3 Elevation Pressure Drop

The elevation pressure drop is based on the relation:

$$\Delta P_E = \overline{\rho} \Delta L \frac{g}{g_c}$$

$$\overline{\rho} = \rho_f (1 - \alpha) + \rho_g \alpha$$

where

ΔP_E = elevation pressure drop

Δ_L = incremental length

$\overline{\rho}$ = average mixture density

g = acceleration of gravity

α = nodal average void fraction

ρ_f, ρ_g = saturated water and vapor density, respectively

Other terms are as previously defined. The TRACG void fraction model is described in Reference 4.4-10. The void fraction model utilized in the core design analysis is described in Reference 4.4-6.

4.4.2.3.4 Acceleration Pressure Drop

A reversible pressure change occurs when an area change is encountered, and an irreversible loss occurs when the fluid is accelerated through the boiling process. The basic formulation for the reversible pressure change resulting from a flow area change in the case of single–phase flow is given by:

$$\Delta P_{ACC} = (1 - \sigma_A^2) \frac{w^2}{2 g_c \rho_f A_2^2}$$

$$\sigma_A = \frac{A_2}{A_1} = \frac{final\ \ flow\ area}{initial\ \ flow\ area}$$

where:

ΔP_{ACC} = acceleration pressure drop

A_2 = final flow area

A_1 = initial flow area

In the case of two–phase flow, the liquid density is replaced by a density ratio so that the reversible pressure change is given by:

$$\Delta P_{ACC} = \left(1-\sigma_A^2\right)\frac{w^2\rho_H}{2g_c\rho_{KE}^2A_2^2}$$

where:

$\frac{1}{\rho_H} = \frac{x}{\rho_g} + \frac{1-x}{\rho_f}$, homogeneous density,

$\frac{1}{\rho_{KE}^2} = \frac{x^3}{\rho_g^2\alpha^2} + \frac{(1-x)^3}{\rho_f^2(1-\alpha)^2}$, kinetic energy density,

α = void fraction at A_2

x = steam quality at A_2

Other terms are as previously defined. The basic formulation for the acceleration pressure change due to density change is:

$$\Delta P_{ACC} = \frac{w^2}{g_c A_{ch}^2}\left[\frac{1}{\rho_{OUT}} - \frac{1}{\rho_{IN}}\right]$$

where ρ is either the homogeneous density, ρ_H, or the momentum density, ρ_M

$$\frac{1}{\rho_M} = \frac{x^2}{\rho_g\alpha} + \frac{(1-x)^2}{\rho_f(1-\alpha)}$$

ρ is evaluated at the inlet and outlet of each axial node. Other terms are as previously defined. The total acceleration pressure drop in boiling water reactors is on the order of a few percent of the total pressure drop. Note that the TRACG model is different for the acceleration pressure drop modeling (see Reference 4.4-10).

4.4.2.3.5 Total Pressure Drop Qualification

The GE14 pressure drop is characterized in Reference 4.4-14. The loss coefficients are qualified against pressure drop test data. The test range includes the operating conditions for the ESBWR. The ESBWR fuel spacer geometry is identical to the design tested in Reference 4.4-14. Because operating conditions and geometry are compatible, the loss coefficients can be applied to the ESBWR. The uncertainty in the core pressure drop is defined by Reference 4.4-9 Section 4.4.1 item C23.

4.4.2.4 Core Coolant Flow Distribution Methods

The core coolant flow distribution methods used in TRACG is described in Reference 4.4-10 Section 6 and 7. TRACG treats all fuel channels as one-dimensional (axial) components, but the vessel is modeled as a three-dimensional component. Hence, the pressure drop across two planes in the vessel is the same at all radial and azimuth locations if the geometry of the components in the vicinity of these planes has radial and azimuth symmetry. Otherwise, this pressure differential displays some (locally) radial and azimuth non-uniformity.

The flow distribution to the fuel assemblies and bypass flow paths in the core simulator model is calculated on the assumption that the pressure drop across all fuel assemblies and bypass flow paths is the same. The bundle pressure drop evaluation includes frictional, local, elevation, and acceleration losses (Sub-sections 4.4.2.3.1 - 4.4.2.3.4). The pressure drop methodology has been qualified to test data (see Reference 4.4-14). The core inlet flow is an input to the core simulator model. The value used was determined based on the TRACG prediction of the natural circulation core inlet flow.

The bypass flow methodology is described in Reference 4.4-10 Section 7.5.1. The same methodology supports the core simulator model.

4.4.2.5 Fuel Heat Transfer Methods

The heat transfer methods used in TRACG is described in the Reference 4.4-10 Section 6 and 7.

The Jens-Lottes (Reference 4.4-7) heat transfer correlation is used in fuel design to determine the cladding-to-coolant heat transfer coefficients for nucleate boiling. The methodology for fuel cladding, gap and pellet heat transfer is described in Section 4.2.

4.4.2.6 Maximum Linear Heat Generation Rate Methods

The Maximum Linear Heat Generation Rate (MLHGR) methods are described in Section 4.2. Margin to design limits for circumferential cladding strain and centerline fuel temperature is evaluated for AOOs in accordance with Reference 4.4-9 Section 4.6.2.1.

4.4.3 Reactor Core Thermal and Hydraulic Evaluations

Typical thermal-hydraulic parameters for the ESBWR are compared to those for a typical BWR/6 plant and the ABWR in Table 4.4-1.

4.4.3.1 Critical Power Evaluations

4.4.3.1.1.1 Bundle Critical Power Performance Evaluation

The bundle critical power performance results are described in Reference 4.4-12. Compliance to steady state MCPR limits is demonstrated for a typical simulation of an equilibrium cycle in Section 4A.

4.4.3.1.1.2 Fuel Cladding Integrity Safety Limit Evaluation

The Fuel Cladding Integrity Safety Limit results are described in Reference 4.4-12. This evaluation includes determination of the uncertainties specific to the ESBWR.

4.4.3.1.1.3 MCPR Operating Limit Evaluation

The MCPR Operating Limit ΔCPR/ICPR results are described in Chapter 15 Section 15.2. The MCPR Operating Limit development including incorporation of the Fuel Cladding Integrity Safety Limit uncertainties is described in Reference 4.4-12.

4.4.3.2 Void Fraction Distribution Evaluations

The axial distribution of core void fractions for the average radial channel and a conservative hot channel as predicted by TRACG are given in Table 4.4-2. The core average and maximum exit values are also provided. Similar distributions for steam quality are given in Table 4.4-3. The core average axial power distribution used to produce these tables is given in Table 4.4-4. The axial distribution, for the channel with the highest exit void fraction for the core reference loading pattern (Figure 4.3-1 and Section 4A), is given in Table 4.4-5.

The expected operating void fraction for the ESBWR is within the qualification basis of the void fraction methods. The void fraction in Table 4-4-2a and 4.4-2b are based on TRACG. The hot channel has a maximum void fraction of 0.92 and assumed a CPR of 1.20. This is conservative compared to the assumed OLMCPR for ESBWR. The void fraction qualification database contains void fractions in excess of 0.92 and covers the void fraction range expected for normal steady state operation as well as AOOs. The core simulator maximum exit void fraction in Table 4.4-5 is 0.90.

The TRACG AOO calculations in Chapter 15 include the consideration of uncertainty in the void fraction.

4.4.3.3 Core Pressure Drop and Hydraulic Loads Evaluations

The expected operating pressure for the ESBWR is within the qualification basis of the pressure drop methods. The TRACG AOO calculations in Chapter 15 include the consideration of uncertainty in the channel pressure drop. The statistical OLMCPR method also assumes pressure drop uncertainty. The impact of uncertainty in core pressure drop is included in the results provided in Reference 4.4-12.

4.4.3.4 Core Coolant Flow Distribution Evaluations

The impact of uncertainty in core flow distribution is included in the results provided in Reference 4.4-12.

4.4.3.5 Fuel Heat Transfer Evaluations

The fuel heat transfer models are included in evaluations described in Section 4.2 and Chapter 15.

4.4.3.6 Maximum Linear Heat Generation Rate Evaluations

The AOO results are described in Chapter 15 Section 15.2. Compliance to steady state MLHGR limits is demonstrated for a typical simulation of an equilibrium cycle in Section 4A.

4.4.4 Description of the Thermal–Hydraulic Design of the Reactor Coolant System

4.4.4.1 Plant Configuration Data

4.4.4.1.1 Reactor Coolant System Configuration

The Reactor Coolant System is described in Chapter 5. The ESBWR reactor coolant system is shown in Figure 5.1-1. The ESBWR design is similar to that of the operating BWRs, except that the recirculation pumps and associated piping are eliminated. Circulation of the reactor coolant

through the ESBWR core is accomplished via natural circulation. The natural circulation flow rate depends on the difference in water density between the downcomer region and the core region. The core flow varies according to the power level, as the density difference changes with changes in power levels. Therefore, a core power-flow map is only a single line and there is no active control of the core flow at any given power level.

4.4.4.1.2 Reactor Coolant System Thermal–Hydraulic Data

The steady-state distribution of temperature, pressure and flow rate for each flow path in the Reactor Coolant System is shown in Figure 1.1-3.

4.4.4.1.3 Reactor Coolant System Geometric Data

Volumes of regions and components within the reactor vessel are shown in Figure 5.1-1. Table 4.4-6 provides the flow path length, height, liquid level, minimum elevations, and flow areas for each major flow path volume within the reactor vessel.

4.4.4.2 Operating Restrictions on Pumps

Not Applicable to the ESBWR. The ESBWR is a natural circulation design.

4.4.4.3 Power/Flow Operating Map

The core power-flow map is only a single line and there is no active control of the core flow at a given power level.

4.4.4.4 Temperature-Power Operating Map

Not Applicable to the ESBWR.

4.4.4.5 Load Following Characteristics

Load following is implemented through the Plant Automation System (PAS). This is described in Chapter 7 Section 7.7.4.

4.4.4.6 Thermal-Hydraulic Characteristics Summary Tables

The thermal-hydraulic characteristics are provided in Table 4.4-1 and Table 4.4-6. The core axial power distributions for the average and hot channels are shown in Table 4.4-4. The axial distribution of core void fractions for the average power channel and the hot channel are given in Table 4.4-2. The core average and core maximum exit void fractions are also provided. Similar distributions for coolant flow quality are provided in Table 4.4-3.

4.4.5 Loose-Parts Monitoring System

The Loose Parts Monitoring System (LPMS) is designed to provide detection of loose metallic parts within the reactor pressure vessel. Detection of loose parts can provide early warning to the operator so that damage to or malfunctions of safety-related primary system components is avoided or mitigated. LPMS detects structure borne sound that can indicate the presence of loose parts impacting against the reactor pressure vessel internals. The system alarms when the signal amplitude exceeds preset limits. The LPMS can evaluate some aspects of selected signals. However, the system by itself does not diagnose the presence and location of a loose part.

Review of LPMS data by an experienced LPM engineer is required to confirm the presence of a loose part.

4.4.5.1 Power Generation Design Bases

The LPMS is designed to provide detection and operator warning of loose parts in the reactor pressure vessel to avoid or mitigate damage to or malfunctions of safety-related primary system components. The LPMS is classified as a non-safety-related system. It is designed in conformance with Regulatory Guide 1.133.

Additional design considerations provide for the inclusion of electronic features to minimize operator-interfacing requirements during normal operation and to enhance the analysis function when operator action is required to investigate potential loose parts.

4.4.5.2 System Description

The LPMS continuously monitors the reactor pressure vessel and appurtenances for indications of loose parts. The LPMS consists of sensors, cables, signal conditioning equipment, alarming monitor, signal analysis and data acquisition equipment, and calibration equipment. The alarm setting after system installation is set low enough to meet the sensitivity requirements, yet is designed to discriminate between normal background noises and the loose part impact signal to minimize spurious alarms. Each sensor channel is isolated to reduce the possibility of signal ground loop problems and to minimize the background noise. Background noises are also minimized by use of tuned filters. A disable signal is provided during control rod movement and other plant maneuvers that may initiate a spurious alert-level alarm.

LPMS sensors are usually accelerometers. The array of LPMS sensors, typically twelve to twenty sensors, is strategically mounted on the external surface of the primary pressure boundary at various elevations and azimuths at natural collection regions for potential loose parts. General mounting locations are at (1) the main steam outlet nozzle, (2) feedwater inlet nozzle, (3) standby liquid control nozzle, and (4) CRD housings. The sensors are mounted in such a fashion as to provide high frequency response and sensitivity.

The online system sensitivity is such that the system meets the calibration requirements of Subsection 4.4.4.5, Test and Inspection. The LPMS frequency range of interest is typically from 1 to 10 kHz. Frequencies lower than 1 kHz are generally associated with flow induced vibration signals or flow noise.

Physical separation is maintained from the sensors at each natural collection region to an area where they are combined and routed through the cable penetration to a termination point. The termination point is selected in the plant where it is accessible for maintenance during full power operation.

The LPMS includes provisions for both automatic and manual start-up of data acquisition equipment with automatic activation in the event the preset alert level is reached or exceeded. The system also initiates an alarm to the control room personnel when an alert condition is reached. The data acquisition system automatically selects the alarmed channel plus additional channels for simultaneous recording. The signal analysis equipment allows immediate visual and audio monitoring of all signals.

Provisions exist for periodic online channel check and functional test and for offline channel calibration during periods of cold shutdown or refueling. The LPMS electronics is designed to facilitate the recognition, location, replacement, repair, and adjustment of malfunctioning LPMS components. The LPMS components located inside the containment have been designed and installed to perform their function following all seismic events that do not require plant shutdown. The LPMS components selected for this application are rated to meet the normal operating radiation, vibration, temperature, and humidity environments in which the components are installed.

All LPMS components within the containment are designed for a 60-year design life. In those instances where a 60-year design life is not practicable, a replacement program is established for those parts that are anticipated to have limited service life.

4.4.5.3 Normal System Operation

The LPMS are set to alarm for detected signals having characteristics of metal-to-metal impacts.

After installation of the sensor array, the LPMS overall and individual channels can be characterized at plant start-up before operation monitoring. Each accelerometer channel exhibits its own particular and unique frequency spectrum. This frequency signature, or background noise, results from a combination of both internal and external sources due to normal and transient conditions.

Calibration is an important part of LPMS operation. The LPMS is calibrated to requirements identified in Subsection 4.4.4.5, Test and Inspection. Alarm level set-point is determined by using a manual calibration device to simulate the presence of a loose part impact near each sensor. The set-point is typically based on a percentage of the calibration signal magnitude, and is a function of actual background noise. Additionally, calibrated impacts at various locations near the sensors assist in diagnosing the source of the signal.

Discrimination logic is typically incorporated in the LPMS to avoid spurious alarms. Discrimination logic rejects events that do not have the characteristics of an impact signal of a loose part. Typical discrimination functions are based on the length of time the signal is above the set-point, the number of channels alarming, the time between alarms, the repetition of the signal, and the waveform and frequency content. False alert signals due to plant maneuvers are avoided by the use of administrative procedures by control room personnel.

Once the loose parts monitor detects an unusual signal characteristic of a metal-to-metal impact, it is essential to determine the source or cause of the alarm. An alarm does not necessarily indicate the presence of a loose part in the reactor. Electrical noises, system malfunctions, limitations in alarm logic, or non-impact noises could cause the alarm. The LPMS detection system is designed to incorporate the discrimination logic to distinguish between an actual loose parts signal and a non-loose parts signal before signaling the control room operator.

Usually the plant operator makes the preliminary evaluation based on the available information. If the presence of unusual metal impact sound is indicated, then the station engineers perform additional evaluation. LPMS experts are required to correctly diagnose the presence and location of a loose part. In order to reach proper conclusions, various factors must be considered such as: plant operating conditions; location of the channels that alarmed; and comparison of the amplitude and frequency contents of the signals with known normal operation data.

4.4.5.4 Safety Evaluation

The LPMS is for use by the plant operator and only for information purposes. The plant operators do not rely on the information provided by the LPMS for the performance of any safety-related action; the LPMS is classified as a non-safety-related system. The LPMS is designed to meet the seismic and environmental operability recommendations of Regulatory Guide 1.133.

4.4.5.5 Test and Inspection

The LPMS is calibrated to detect a metallic loose part that impacts on the inside surface of the reactor pressure vessel within the maximum proximity of a sensor. Provision is made to verify the calibration of the LPMS at each refueling. The system is recalibrated as necessary when found to be out of calibration. A test and reset capability is included for functional test capability.

The manufacturer provides services of qualified personnel to provide technical guidance for installation, start-up, and acceptance testing of the system. In addition, the manufacturer provides the necessary training of plant personnel for proper system operation and maintenance and planned operating and record-keeping procedures.

4.4.5.6 Instrumentation Application

The LPMS consists of sensors, cables, signal conditioning equipment, alarming monitor, signal analysis and data acquisition equipment, and calibration equipment.

4.4.6 Testing and Verification

The testing and verification techniques to be used to assure that the planned thermal and hydraulic design characteristics of the core have been provided, and remain within required limits throughout core lifetime, are discussed in Chapter 14.

4.4.7 COL Information

4.4.7.1 Reactor Core Thermal and Hydraulic Design

This section contains no requirement for additional information to be provided in support of the combined license. Combined License applicants referencing the ESBWR certified design would address changes to the thermal-hydraulic design of the reactor coolant system or loose parts monitoring system, if different from that presented in the DCD.

4.4.8 References

4.4-1 General Electric Company, “Core Flow Distribution in a Modern Boiling Water Reactor as Measured in Monticello,” NEDO-10299A, October 1976.

4.4-2 General Electric Company, “Core Flow Distribution in a General Electric Boiling Water Reactor as Measured in Quad Cities Unit 1,” NEDO-10722A, August 1976.

4.4-3 General Electric Company, “Brunswick Steam Electric Plant Unit 1 Safety Analysis Report for Plant Modifications to Eliminate Significant In-Core Vibrations,” NEDO-21215, March 1976.

4.4-4 R. C. Martinelli and D.E. Nelson, "Prediction of Pressure Drops During Forced Convection Boiling of Water," ASME Trans., 70, 695-702, 1948.

4.4-5 C. J. Baroczy, "A Systematic Correlation for Two-Phase Pressure Drop," Heat Transfer Conference (Los Angeles), AICLE, Preprint No. 37, 1966.

4.4-6 N. Zuber and J. A. Findlay, "Average Volumetric Concentration in Two-Phase Flow Systems," Transactions of the ASME Journal of Heat Transfer, November 1965.

4.4-7 USAEC, W. H. Jens and P. A. Lottes, "Analysis of Heat Transfer, Burnout, Pressure Drop and Density Data for High Pressure Water," USAEC Report- 4627, 1972.

4.4-8 General Electric Company, "General Electric BWR Thermal Analysis Basis (GETAB): Data Correlation and Design Application," NEDO-10958-A, January 1977.

4.4-9 GE Nuclear Energy, "TRACG Application for ESBWR," NEDE-33083P-A Revision 0, Class III (proprietary), March 2005.

4.4-10 GE Nuclear Energy, "Licensing Topical Report TRACG Model Description," NEDE-32176P Revision 2, Class III (proprietary), December 1999.

4.4-11 GE Nuclear Energy, "Licensing Topical Report TRACG Qualification," NEDE-32177P Revision 2, Class III (proprietary), January 2000.

4.4-12 GE Nuclear Energy, "GE14 for ESBWR Critical Power Correlation, Uncertainty, and OLMCPR Development", NEDC-33237 P, Class III (proprietary), to be issued

4.4-13 GE Nuclear Energy, "Methodology and Uncertainties for Safety Limit MCPR Evaluations", NEDC–32601P-A, Class III (proprietary), August 1999.

4.4-14 GE Nuclear Energy, "GE14 Pressure Drop Characteristics", NEDC-33238P, Class III (proprietary), to be issued

Table 4.4-1a

Typical Thermal–Hydraulic Design Characteristics of the Reactor Core (SI Units)

General Operating Conditions	BWR/6	ABWR	ESBWR
Reference design thermal output (MWt)	3579	3926	4500
Power level for engineered safety features (MWt)	3730	4005	4590
Steam flow rate, at 420°F final feedwater temperature (kg/s)	1940	2122	2433
Core coolant flow rate (kg/s)	13104	14502	9034-10584
Feedwater flow rate (kg/s)	1936	2118	2451
System pressure, nominal in steam dome (kPa)	7171	7171	7171
System pressure, nominal core design (kPa)	7274	7274	7240
Coolant saturation temperature at core design pressure (°C)	288	288	288
Average power density (kW/L)	54.1	50.6	54.3
Core total heat transfer area (m2)	6810	7727	9976
Core inlet enthalpy (kJ/kg)	1227	1227	1183-1197
Core inlet temperature (°C)	278	278	270-272
Core maximum exit voids within assemblies (%)	79.0	75.1	91.6
Core average void fraction, active coolant	0.414	0.408	0.320
Active coolant flow area per assembly (m^2)	0.0098	0.0101	0.0093
Core average inlet velocity (m/s)	2.13	1.96	1.12
Maximum inlet velocity (m/s)	2.60	26.7	1.15
Total core pressure drop (kPa)	182.0	168.2	70.0
Core support plate pressure drop (kPa)	151.7	137.9	41.3
Average orifice pressure drop, central region (kPa)	39.4	60.3	20.3
Average orifice pressure drop, peripheral region (kPa)	129	122	37.1
Maximum channel pressure loading (kPa)	106	75.2	24.4
Average-power assembly channel pressure loading (bottom) (kPa)	97.2	65.5	21.5
Shroud support ring and lower shroud pressure loading (kPa)	177	165	7.4
Upper shroud pressure loading (kPa)	25.5	24.1	17.4

Table 4.4-1b

Typical Thermal–Hydraulic Design Characteristics of the Reactor Core (English Units)

General Operating Conditions	BWR/6	ABWR	ESBWR
Reference design thermal output (MWt)	3579	3926	4500
Power level for engineered safety features (MWt)	3730	4005	4590
Steam flow rate, at 420°F final feedwater temperature (Mlb/hr)	15.40	16.84	19.31
Core coolant flow rate (Mlb/hr)	104.0	115.1	71.7-84.0
Feedwater flow rate (Mlb/hr)	15.4	16.8	19.5
System pressure, nominal in steam dome (psia)	1040	1040	1040
System pressure, nominal core design (psia)	1055	1055	1050
Coolant saturation temperature at core design pressure (°F)	551	551	550.6
Average power density (kW/L)	54.1	50.6	54.3
Core total heat transfer area (ft2)	73,303	83,176	107,376
Core inlet enthalpy (Btu/lb)	527.7	527.6	508.7-514.7
Core inlet temperature (°F)	533	533	517.5-522.4
Core maximum exit voids within assemblies (%)	79.0	75.1	91.6
Core average void fraction, active coolant	0.41	0.41	0.32
Active coolant flow area per assembly ($in.^2$)	15.2	15.7	14.4
Core average inlet velocity (ft/sec)	7.0	6.4	3.7
Maximum inlet velocity (ft/sec)	8.5	7.5	3.8
Total core pressure drop (psi)	26.4	24.4	10.2
Core support plate pressure drop (psi)	22	20	6.0
Average orifice pressure drop, central region (psi)	5.7	8.8	2.9
Average orifice pressure drop, peripheral region (psi)	18.7	17.7	5.4
Maximum channel pressure loading (psi)	15.40	10.9	3.5
Average-power assembly channel pressure loading (bottom) (psi)	14.1	9.5	3.1
Shroud support ring and lower shroud pressure loading	25.7	23.9	1.1
Upper shroud pressure loading (psi)	3.7	3.5	2.5

Table 4.4-2a

Void Distribution for Analyzed Core –TRACG Average Channel

Channel Power =4.427 MW, CPR = 1.67
Core Average Value = 0.32
Maximum Core Exit Value = 0.83
Active Fuel Length = 3.048 m / 120.00 inches

Node (m above BAF)	Average Node Value	Node (m above BAF)	Average Node Value
1 (BAF+0.02)	0.00	17 (BAF+0.69)	0.40
2 (BAF+0.06)	0.00	18 (BAF+0.84)	0.49
3 (BAF+0.10)	0.00	19 (BAF+0.99)	0.57
4 (BAF+0.13)	0.00	20 (BAF+1.14)	0.63
5 (BAF+0.17)	0.01	21 (BAF+1.30)	0.68
6 (BAF+0.21)	0.02	22 (BAF+1.45)	0.71
7 (BAF+0.25)	0.04	23 (BAF+1.60)	0.73
8 (BAF+0.29)	0.07	24 (BAF+1.75)	0.74
9 (BAF+0.32)	0.10	25 (BAF+1.91)	0.75
10 (BAF+0.36)	0.12	26 (BAF+2.06)	0.77
11 (BAF+0.40)	0.15	27 (BAF+2.21)	0.79
12 (BAF+0.44)	0.18	28 (BAF+2.36)	0.80
13 (BAF+0.48)	0.21	29 (BAF+2.51)	0.82
14 (BAF+0.51)	0.23	30 (BAF+2.67)	0.83
15 (BAF+0.55)	0.26	31 (BAF+2.82)	0.83
16 (BAF+0.59)	0.29	32 (BAF+2.97)	0.83

Table 4.4-2b

Void Distribution for Analyzed Core – TRACG Hot Channel

Channel Power = 5.817 MW, CPR = 1.20
Core Average Value = 0.32
Maximum Core Exit Value = 0.92
Active Fuel Length = 3.048 m / 120.00 inches

Node (m above BAF)	Average Node Value	Node (m above BAF)	Average Node Value
1 (BAF+0.02)	0.00	17 (BAF+0.69)	0.59
2 (BAF+0.06)	0.00	18 (BAF+0.84)	0.67
3 (BAF+0.10)	0.00	19 (BAF+0.99)	0.72
4 (BAF+0.13)	0.02	20 (BAF+1.14)	0.74
5 (BAF+0.17)	0.04	21 (BAF+1.30)	0.75
6 (BAF+0.21)	0.07	22 (BAF+1.45)	0.78
7 (BAF+0.25)	0.11	23 (BAF+1.60)	0.81
8 (BAF+0.29)	0.15	24 (BAF+1.75)	0.84
9 (BAF+0.32)	0.19	25 (BAF+1.91)	0.86
10 (BAF+0.36)	0.23	26 (BAF+2.06)	0.88
11 (BAF+0.40)	0.27	27 (BAF+2.21)	0.89
12 (BAF+0.44)	0.31	28 (BAF+2.36)	0.90
13 (BAF+0.48)	0.35	29 (BAF+2.51)	0.91
14 (BAF+0.51)	0.39	30 (BAF+2.67)	0.92
15 (BAF+0.55)	0.43	31 (BAF+2.82)	0.91
16 (BAF+0.59)	0.46	32 (BAF+2.97)	0.92

Table 4.4-3a

Flow Quality Distribution for Analyzed Core – TRACG Average Channel

Core Average Value = 0.10
Maximum Core Exit Value = 0.29
Active Fuel Length = 3.048 m / 120.00 inches

Node (m above BAF)	Average Node Value	Node (m above BAF)	Average Node Value
1 (BAF+0.02)	0.00	17 (BAF+0.69)	0.05
2 (BAF+0.06)	0.00	18 (BAF+0.84)	0.07
3 (BAF+0.10)	0.00	19 (BAF+0.99)	0.09
4 (BAF+0.13)	0.00	20 (BAF+1.14)	0.11
5 (BAF+0.17)	0.00	21 (BAF+1.30)	0.13
6 (BAF+0.21)	0.00	22 (BAF+1.45)	0.16
7 (BAF+0.25)	0.00	23 (BAF+1.60)	0.18
8 (BAF+0.29)	0.00	24 (BAF+1.75)	0.20
9 (BAF+0.32)	0.01	25 (BAF+1.91)	0.22
10 (BAF+0.36)	0.01	26 (BAF+2.06)	0.23
11 (BAF+0.40)	0.01	27 (BAF+2.21)	0.25
12 (BAF+0.44)	0.01	28 (BAF+2.36)	0.27
13 (BAF+0.48)	0.02	29 (BAF+2.51)	0.28
14 (BAF+0.51)	0.02	30 (BAF+2.67)	0.29
15 (BAF+0.55)	0.02	31 (BAF+2.82)	0.29
16 (BAF+0.59)	0.03	32 (BAF+2.97)	0.29

Table 4.4-3b

Flow Quality Distribution for Analyzed Core – TRACG Hot Channel

Core Average Value = 0.10
Maximum Core Exit Value = 0.44
Active Fuel Length = 3.048 m / 120.00 inches

Node (m above BAF)	Average Node Value	Node (m above BAF)	Average Node Value
1 (BAF+0.02)	0.00	17 (BAF+0.69)	0.10
2 (BAF+0.06)	0.00	18 (BAF+0.84)	0.13
3 (BAF+0.10)	0.00	19 (BAF+0.99)	0.16
4 (BAF+0.13)	0.00	20 (BAF+1.14)	0.20
5 (BAF+0.17)	0.00	21 (BAF+1.30)	0.23
6 (BAF+0.21)	0.00	22 (BAF+1.45)	0.26
7 (BAF+0.25)	0.01	23 (BAF+1.60)	0.29
8 (BAF+0.29)	0.01	24 (BAF+1.75)	0.32
9 (BAF+0.32)	0.01	25 (BAF+1.91)	0.35
10 (BAF+0.36)	0.02	26 (BAF+2.06)	0.37
11 (BAF+0.40)	0.02	27 (BAF+2.21)	0.40
12 (BAF+0.44)	0.03	28 (BAF+2.36)	0.42
13 (BAF+0.48)	0.04	29 (BAF+2.51)	0.44
14 (BAF+0.51)	0.05	30 (BAF+2.67)	0.45
15 (BAF+0.55)	0.05	31 (BAF+2.82)	0.44
16 (BAF+0.59)	0.06	32 (BAF+2.97)	0.44

Table 4.4-4a

Axial Power Distribution Used to Generate Void and Quality for Analyzed Core - TRACG Average Channel

Node (m above BAF)	Average Node Value	Node (m above BAF)	Average Node Value
1 (BAF+0.02)	0.58	17 (BAF+0.69)	1.28
2 (BAF+0.06)	0.58	18 (BAF+0.84)	1.26
3 (BAF+0.10)	0.58	19 (BAF+0.99)	1.24
4 (BAF+0.13)	1.02	20 (BAF+1.14)	1.22
5 (BAF+0.17)	1.13	21 (BAF+1.30)	1.20
6 (BAF+0.21)	1.13	22 (BAF+1.45)	1.16
7 (BAF+0.25)	1.23	23 (BAF+1.60)	1.10
8 (BAF+0.29)	1.30	24 (BAF+1.75)	1.04
9 (BAF+0.32)	1.30	25 (BAF+1.91)	0.88
10 (BAF+0.36)	1.31	26 (BAF+2.06)	0.80
11 (BAF+0.40)	1.33	27 (BAF+2.21)	0.73
12 (BAF+0.44)	1.33	28 (BAF+2.36)	0.65
13 (BAF+0.48)	1.32	29 (BAF+2.51)	0.53
14 (BAF+0.51)	1.31	30 (BAF+2.67)	0.40
15 (BAF+0.55)	1.31	31 (BAF+2.82)	0.26
16 (BAF+0.59)	1.31	32 (BAF+2.97)	0.14

Table 4.4-4b

Axial Power Distribution Used to Generate Void and Quality for Analyzed Core - TRACG Hot Channel

Node (m above BAF)	Average Node Value	Node (m above BAF)	Average Node Value
1 (BAF+0.02)	0.58	17 (BAF+0.69)	1.28
2 (BAF+0.06)	0.58	18 (BAF+0.84)	1.26
3 (BAF+0.10)	0.58	19 (BAF+0.99)	1.24
4 (BAF+0.13)	1.02	20 (BAF+1.14)	1.22
5 (BAF+0.17)	1.13	21 (BAF+1.30)	1.20
6 (BAF+0.21)	1.13	22 (BAF+1.45)	1.16
7 (BAF+0.25)	1.23	23 (BAF+1.60)	1.10
8 (BAF+0.29)	1.30	24 (BAF+1.75)	1.04
9 (BAF+0.32)	1.30	25 (BAF+1.91)	0.88
10 (BAF+0.36)	1.31	26 (BAF+2.06)	0.80
11 (BAF+0.40)	1.33	27 (BAF+2.21)	0.73
12 (BAF+0.44)	1.33	28 (BAF+2.36)	0.65
13 (BAF+0.48)	1.32	29 (BAF+2.51)	0.53
14 (BAF+0.51)	1.31	30 (BAF+2.67)	0.40
15 (BAF+0.55)	1.31	31 (BAF+2.82)	0.26
16 (BAF+0.59)	1.31	32 (BAF+2.97)	0.14

Table 4.4-5

Axial Distribution for Typical Core – Core Simulator Hot Channel

Channel Power = 5.316 MW, CPR = 1.50
Maximum Core Exit Value = 0.90
Active Fuel Length = 3.048 m / 120.00 inches

Node (m above BAF)	Axial Power Factor	Void Fraction
1 (BAF+0.06)	0.63	0.00
2 (BAF+0.18)	1.22	0.02
3 (BAF+0.30)	1.49	0.13
4 (BAF+0.43)	1.53	0.30
5 (BAF+0.55)	1.49	0.43
6 (BAF+0.67)	1.42	0.52
7 (BAF+0.79)	1.35	0.59
8 (BAF+0.91)	1.30	0.65
9 (BAF+1.04)	1.25	0.69
10 (BAF+1.16)	1.22	0.72
11 (BAF+1.28)	1.18	0.74
12 (BAF+1.40)	1.15	0.76
13 (BAF+1.52)	1.12	0.78
14 (BAF+1.65)	1.09	0.80
15 (BAF+1.77)	1.06	0.82
16 (BAF+1.89)	1.00	0.83
17 (BAF+2.01)	0.95	0.84
18 (BAF+2.13)	0.90	0.86
19 (BAF+2.26)	0.83	0.87
20 (BAF+2.38)	0.75	0.87
21 (BAF+2.50)	0.65	0.88
22 (BAF+2.62)	0.54	0.89
23 (BAF+2.74)	0.42	0.89
24 (BAF+2.87)	0.29	0.89
25 (BAF+2.99)	0.16	0.90

Table 4.4-6

ESBWR Reactor Coolant System Geometric Data

	Flow Path Length (m)	Height and Liquid Level (m)	Elevation of Bottom of Volume (m^3)	Average Flow Area (m^2)
Lower Plenum	4.13 (Axial)) 1.78 (Radial)	4.13/4.13	0.000	16.83
Core	3.79	3.77/2-Phase	4.13	20.22
Chimney	6.61	6.61/2-Phase	7.90	29.27
Upper Plenum	2.75	2.75/2-Phase	14.51	29.53
Dome	1.78 (Radial) 2.79 (Axial)	2.79/Steam	24.77	28.67
Downcomer	14.53	14.53/14.53	2.74	8.40